



## Towards improved monitoring of offshore carbon storage: A real-world field experiment detecting a controlled sub-seafloor CO<sub>2</sub> release

Anita Flohr<sup>a,b,\*</sup>, Allison Schaap<sup>b,\*</sup>, Eric P. Achterberg<sup>c</sup>, Guttorm Alendal<sup>d</sup>, Martin Arundell<sup>b</sup>, Christian Berndt<sup>c</sup>, Jerry Blackford<sup>e</sup>, Christoph Böttner<sup>c</sup>, Sergey M. Borisov<sup>f</sup>, Robin Brown<sup>b</sup>, Jonathan M. Bull<sup>a</sup>, Liam Carter<sup>b</sup>, Baixin Chen<sup>g</sup>, Andrew W. Dale<sup>c</sup>, Dirk de Beer<sup>h</sup>, Marcella Dean<sup>i</sup>, Christian Deusner<sup>c</sup>, Marius Dewar<sup>e,g</sup>, Jennifer M. Durden<sup>b</sup>, Saskia Elsen<sup>c</sup>, Mario Esposito<sup>c</sup>, Michael Faggetter<sup>a</sup>, Jan P. Fischer<sup>j</sup>, Amine Gana<sup>b</sup>, Jonas Gros<sup>c</sup>, Matthias Haeckel<sup>c</sup>, Rudolf Hanz<sup>b</sup>, Moritz Holtappels<sup>k</sup>, Brett Hosking<sup>b</sup>, Veerle A.I. Huvenne<sup>b</sup>, Rachael H. James<sup>a</sup>, Dirk Koopmans<sup>h</sup>, Elke Kossel<sup>c</sup>, Timothy G. Leighton<sup>a</sup>, Jianghui Li<sup>a</sup>, Anna Lichtschlag<sup>b</sup>, Peter Linke<sup>c</sup>, Socratis Loucaides<sup>b</sup>, María Martínez-Cabanas<sup>c</sup>, Juerg M. Matter<sup>a</sup>, Thomas Mesher<sup>e</sup>, Samuel Monk<sup>a,b</sup>, Matthew Mowlem<sup>a,b</sup>, Anna Oleynik<sup>d</sup>, Stathys Papadimitriou<sup>b</sup>, David Paxton<sup>b</sup>, Christopher R. Pearce<sup>b</sup>, Kate Peel<sup>b</sup>, Ben Roche<sup>a</sup>, Henry A. Ruhl<sup>b,l</sup>, Umer Saleem<sup>g</sup>, Carla Sands<sup>b</sup>, Kevin Saw<sup>b</sup>, Mark Schmidt<sup>c</sup>, Stefan Sommer<sup>c</sup>, James A. Strong<sup>b</sup>, Jack Triest<sup>m</sup>, Birgit Ungerböck<sup>f,j</sup>, John Walk<sup>b</sup>, Paul White<sup>a</sup>, Steve Widdicombe<sup>e</sup>, Robert Euan Wilson<sup>b</sup>, Hannah Wright<sup>b</sup>, James Wyatt<sup>b</sup>, Douglas Connelly<sup>b</sup>

<sup>a</sup> University of Southampton, Waterfront Campus, European Way, Southampton, SO14 3ZH, UK

<sup>b</sup> National Oceanography Centre, European Way, Southampton, SO14 3ZH, UK

<sup>c</sup> GEOMAR Helmholtz Centre for Ocean Research Kiel, Wischhofstr. 1-3, 24148 Kiel, Germany

<sup>d</sup> University of Bergen, Department of Mathematics, Realfagbygget, Allégt. 41, 5020 Bergen, Norway

<sup>e</sup> Plymouth Marine Laboratory, Prospect Place, Plymouth, PL1 3DH, UK

<sup>f</sup> Graz University of Technology, Rechbauerstraße 12, 8010 Graz, Austria

<sup>g</sup> Heriot-Watt University, Edinburgh, EH14 4AS, UK

<sup>h</sup> Max Planck Institute for Marine Microbiology, Celsiusstr. 1, 28359 Bremen, Germany

<sup>i</sup> Shell Global Solutions International BV, Grasweg 31, 1031 HW Amsterdam, the Netherlands

<sup>j</sup> Pyroscience GmbH, Hubertusstr. 35, 52064 Aachen, Germany

<sup>k</sup> Alfred Wegener Institute, Am Handelshafen 12, 27570 Bremerhaven, Germany

<sup>l</sup> Monterey Bay Aquarium Research Institute, Moss Landing, 95010, USA

<sup>m</sup> 4H-JENA Engineering GmbH, Jena, Germany<sup>2</sup>

### ARTICLE INFO

#### Keywords:

Offshore carbon storage  
Carbon dioxide capture and storage (CCS)  
Marine field experiment  
Monitoring  
CO<sub>2</sub> leakage  
Attribution, detection and quantification

### ABSTRACT

Carbon capture and storage (CCS) is a key technology to reduce carbon dioxide (CO<sub>2</sub>) emissions from industrial processes in a feasible, substantial, and timely manner. For geological CO<sub>2</sub> storage to be safe, reliable, and accepted by society, robust strategies for CO<sub>2</sub> leakage detection, quantification and management are crucial. The STEMM-CCS (Strategies for Environmental Monitoring of Marine Carbon Capture and Storage) project aimed to provide techniques and understanding to enable and inform cost-effective monitoring of CCS sites in the marine environment. A controlled CO<sub>2</sub> release experiment was carried out in the central North Sea, designed to mimic an unintended emission of CO<sub>2</sub> from a subsurface CO<sub>2</sub> storage site to the seafloor. A total of 675 kg of CO<sub>2</sub> were released into the shallow sediments (~3 m below seafloor), at flow rates between 6 and 143 kg/d. A combination of novel techniques, adapted versions of existing techniques, and well-proven standard techniques were used to

\* Corresponding authors.

E-mail addresses: [anita.flohr@noc.ac.uk](mailto:anita.flohr@noc.ac.uk) (A. Flohr), [allison.schaap@noc.ac.uk](mailto:allison.schaap@noc.ac.uk) (A. Schaap).

<sup>1</sup> These authors contributed equally.

<sup>2</sup> previously Kongsberg Maritime Contros GmbH, Kiel, Germany.

detect, characterise and quantify gaseous and dissolved CO<sub>2</sub> in the sediments and the overlying seawater. This paper provides an overview of this ambitious field experiment. We describe the preparatory work prior to the release experiment, the experimental layout and procedures, the methods tested, and summarise the main results and the lessons learnt.

## 1. Introduction

Human activities, including fossil fuel burning, land-use changes, and cement manufacture, have caused the atmospheric carbon dioxide (CO<sub>2</sub>) concentration to rise from a pre-industrial level of 277 parts per million (ppm) to a current level of ~412 ppm in 2020 (e.g., Friedlingstein et al., 2019; Dlugokencky and Tans, 2020). This atmospheric accumulation of anthropogenic CO<sub>2</sub> has been linked to the rise of the global mean temperature, presently approximately 1.0 °C above pre-industrial levels (IPCC, 2018). The United Nations Framework Convention on Climate Change (UNFCCC) agreed to take action and to keep global warming below 1.5–2 °C above pre-industrial levels (UNFCCC, 2015; IPCC, 2014, 2018). CO<sub>2</sub> capture and storage (CCS) is a key technology in many of the recent mitigation scenarios that would meet this goal (IPCC, 2005, 2018). CCS involves the capture of CO<sub>2</sub> – principally from large point sources such as industrial power plants – and its injection into geological storage formations such as deep saline aquifers or depleted oil and gas reservoirs for permanent storage (IPCC, 2005). Compared to other CO<sub>2</sub> mitigation strategies, such as improving energy efficiency and use of renewable energy, the crucial benefit of CCS lies in its potential to significantly (at giga-tonne scale) and rapidly reduce CO<sub>2</sub> emissions while making use of infrastructure that already exists for oil and gas production (IPCC, 2005).

It is estimated that the majority of Western Europe's potential CO<sub>2</sub> storage capacity is located offshore (IEAGHG, 2008; Vangkilde-Pederson, 2009). There are a small number of active (Sleipner, North Sea, Norway; Snøhvit, Barents Sea, Norway) and completed (K12-B, North Sea, Netherlands) offshore CO<sub>2</sub> injection projects in Europe that provide confidence in the performance of offshore gas injection and storage (Vandeweyer et al., 2011; Hansen et al., 2013; Van der Meer, 2013; Furre et al., 2017; Ringrose and Meckel, 2019). These and previous CO<sub>2</sub> storage demonstration projects have improved our understanding of the strengths and development needs of various monitoring approaches (IEAGHG, 2008, 2012, 2015; Dixon and Romanak, 2015; Jenkins et al., 2015).

Leakage of injected CO<sub>2</sub> from well-selected, designed and managed geological storage sites back into the atmosphere is generally considered unlikely (IPCC, 2005). However, robust strategies for leak detection and management of offshore CCS projects are a regulatory requirement to comply with international marine legislation (e.g., EU CCS Directive (EU, 2009), London Protocol (IMO, 2006) and OSPAR Convention (OSPAR, 2007)), and are essential for public acceptance of CCS as a safe and reliable technology for the long-term mitigation of elevated anthropogenic CO<sub>2</sub> emissions (e.g., Mabon et al., 2014, 2015, 2017).

Previous research projects, including ECO<sub>2</sub> (Sub-seabed CO<sub>2</sub> Storage: Impact on Marine Ecosystems), QICS (Quantifying and Monitoring Potential Ecosystem of Geological Carbon Storage) and ETI MMV (Energy Technologies Institute Measurement, Monitoring and Verification of CO<sub>2</sub> Storage), have advanced technologies for detection of leakage at the seafloor and have improved knowledge of the local impacts that CO<sub>2</sub> leakage may have on marine ecosystems (Blackford et al., 2014, 2015; Jones et al., 2015; Taylor et al., 2015). Building on this, an overall aim of the Strategies for Environmental Monitoring of Marine Carbon Capture and Storage (STEMM-CCS) project was to deliver new approaches, methodologies and tools for cost-effective environmental monitoring and leakage quantification at offshore CO<sub>2</sub> storage sites.

The specific aims of the STEMM-CCS project were to:

- develop new tools and techniques for the monitoring, quantification, and assessment of a potential CO<sub>2</sub> leakage from an offshore CO<sub>2</sub> storage site;
- demonstrate the suitability of these tools and techniques in a representative field experiment mimicking a CO<sub>2</sub> leakage from a sub-seafloor CO<sub>2</sub> storage site;
- demonstrate a CCS-specific implementation of an ecological baseline measurement, incorporating physical, chemical and biological variability;
- understand the role of natural geological and artificial features as potential pathways for subsurface CO<sub>2</sub> migration;
- develop and evaluate modelling tools to inform monitoring strategies and provide a framework to interpret the experimental results, and translate them to other settings.

To achieve these aims, the STEMM-CCS project conducted a unique CO<sub>2</sub> release experiment designed to mimic a CO<sub>2</sub> leakage from an offshore CO<sub>2</sub> storage site and to demonstrate and evaluate existing and new approaches for characterising and quantifying this release. To enable this, a controlled mixture of CO<sub>2</sub> and tracer gases was released into the sediments at 3 m below the seafloor. A range of novel and standard methods were applied to detect and characterise the release of CO<sub>2</sub> (Fig. 1). The field experiment involved two research vessels and was carried out in the British sector of the central North Sea during 27 April - 27 May 2019.

This paper provides a detailed overview of this field experiment and an introduction to the STEMM-CCS special issue by summarising (i) the preparatory and baseline work that was conducted prior to the release experiment, (ii) the experimental set up and the methods evaluated, and (iii) the main results and the lessons learnt. For detailed results, the reader is referred to the specific papers published as part of this special issue.

### 1.1. Experiment location and setup

#### 1.1.1. Experiment location

The STEMM-CCS experimental CO<sub>2</sub> release was conducted within the surface sediments overlying the proposed Goldeneye CO<sub>2</sub> storage reservoir, a depleted gas condensate field situated offshore from Scotland in the Outer Moray Firth, in the British sector of the central North Sea (56–60 °N) (Dean and Tucker, 2017) (Fig. 2). Located in a sandstone formation of the Lower Cretaceous (Albian-Aptian) period, the reservoir is 10–15 km wide and 60–90 m thick (e.g., Law et al., 2000).

The Goldeneye reservoir was discovered in 1996 and produced 16 × 10<sup>9</sup> m<sup>3</sup> of gas and 23 million barrels of condensate after production by Shell commenced in 2004 (Wilson et al., 2005; Shell, 2015). After gas production ended in 2011, the depleted reservoir was identified as a potential CO<sub>2</sub> storage site for the Peterhead CCS demonstration project. This project was envisaged to capture CO<sub>2</sub> from the Peterhead power plant with subsequent injection of about 15 million tonnes of CO<sub>2</sub> into the depleted Goldeneye reservoir (Shell, 2015; Cotton et al., 2017; Dean and Tucker, 2017). The Peterhead CCS demonstration project was cancelled after the withdrawal of funding by the UK government in 2015 (Dean and Tucker, 2017). The associated scientific research projects STEMM-CCS and CHIMNEY went ahead nonetheless, to underpin the scientific and technological developments necessary for other or future subsea CO<sub>2</sub> storage work. The CHIMNEY project (Characterisation of Major Overburden Leakage Pathways above Sub-sea floor CO<sub>2</sub> Storage Reservoirs in the North Sea; <https://www.southampton.ac.uk/oes/res>

earch/projects/chimney.page) developed new techniques to predict natural and anthropogenically-induced permeability of the reservoir overburden, including intensive studies of naturally occurring “seismic chimney” structures. While this paper focusses on the in-situ release experiment, the paper by Robinson et al. (2020) examines the work done from a geophysical perspective.

### 1.1.2. Permissions and legal considerations for the CO<sub>2</sub> release experiment

Any work in the Scottish sector of the North Sea requires permission from Marine Scotland, the statutory body of the Scottish Government responsible for the protection of Scotland’s coastal waters and sea. Acquiring the required authorisation for the STEMM-CCS experiment was complex because injecting CO<sub>2</sub> into the seabed could be viewed as ocean dumping. Following consultation with OSPAR representatives, the experiment was designated as placement of tracers (CO<sub>2</sub> was considered a tracer in this context) below the seabed. Following the submission of the application for the controlled CO<sub>2</sub> release experiment, there was a three-month public consultation period after which the license for the work was published. In addition, Crown Estate Scotland conducted a spatial conflict check, because a commercial company had been granted a license for future storage of CO<sub>2</sub> in the Goldeneye reservoir. Crown Estate identified no conflicts. Consequently, since there was no storage of CO<sub>2</sub>, no permanent presence, and no conflict with other users on the seabed, permission was granted. The permit allowed the limited release of up to 3 tonnes of CO<sub>2</sub> with associated tracers; we released just over 20 % of this. In addition, a model was developed and executed that showed the limited spatial and temporal impact the release would have on the environment, given the low quantity of gas released and the impact of dilution from tidal flushing. Prior to, and periodically during the release experiment, a trained marine mammal observer performed regular surveys from the ship. This was required due to concerns around the use of acoustic sensor-based systems.

### 1.1.3. Baseline

To differentiate with confidence between CO<sub>2</sub> leakage and any natural variability in the local environment, monitoring needs to be supported by a robust baseline (OSPAR, 2007; EU, 2009; IEAGHG, 2012,

2015), which provides a longer-term picture of the regional spatio-temporal variability. This is in contrast to “background measurements”, which refers here to samples taken at non-affected sites near the experimental release site during the experiment. STEMM-CCS therefore conducted baseline surveys to characterise the spatio-temporal variability of all relevant processes in the region and to provide a basis against which anomalies could be identified. Guided by knowledge gained from the precursor project QICS (Blackford et al., 2014), STEMM-CCS aimed to provide best practice optimisation for creating ecological and environmental baselines for offshore CO<sub>2</sub> storage sites. To this end, two baseline cruises to the Goldeneye site were coordinated by GEOMAR Helmholtz Centre for Ocean Research Kiel: cruise number POS518 in October 2017 and cruise number POS527 in August 2018, both aboard RV *Poseidon* (Table 1). The main goals were to deploy baseline landers for continuous physical and biogeochemical measurements prior to the release experiment and to take samples for further characterisation of the water column, the sediments and the benthic communities (Section 2). Additional background work was carried out prior to and throughout the CO<sub>2</sub> injection during the JC180 and POS534 cruises (Section 2).

### 1.2. Behaviour of CO<sub>2</sub> in the marine environment

When CO<sub>2</sub> is injected into marine sediments, part of it remains in the gas phase, where it either accumulates in gas pockets within the sediments or percolates through the sediments to the seabed where it emerges as bubbles that rapidly dissolve in the overlying seawater (e.g., McGinnis et al., 2011; Gros et al., 2019; Vielstädte et al., 2019). When CO<sub>2</sub> dissolves in seawater, it forms carbonic acid (H<sub>2</sub>CO<sub>3</sub>) that subsequently dissociates to form bicarbonate (HCO<sub>3</sub><sup>-</sup>) and carbonate (CO<sub>3</sub><sup>2-</sup>) ions. The total concentration of dissolved CO<sub>2</sub> in seawater is therefore given by the sum of the concentrations of H<sub>2</sub>CO<sub>3</sub>, HCO<sub>3</sub><sup>-</sup>, and CO<sub>3</sub><sup>2-</sup>, which is referred to as dissolved inorganic carbon (DIC) (Zeebe and Wolf-Gladrow, 2001). Some part of the CO<sub>2</sub> gas also dissolves and potentially reacts with the sediment pore waters (i.e., the water surrounding the solid sediment particles), increasing the DIC content of the pore waters. During the in-situ release experiment, a wide range of

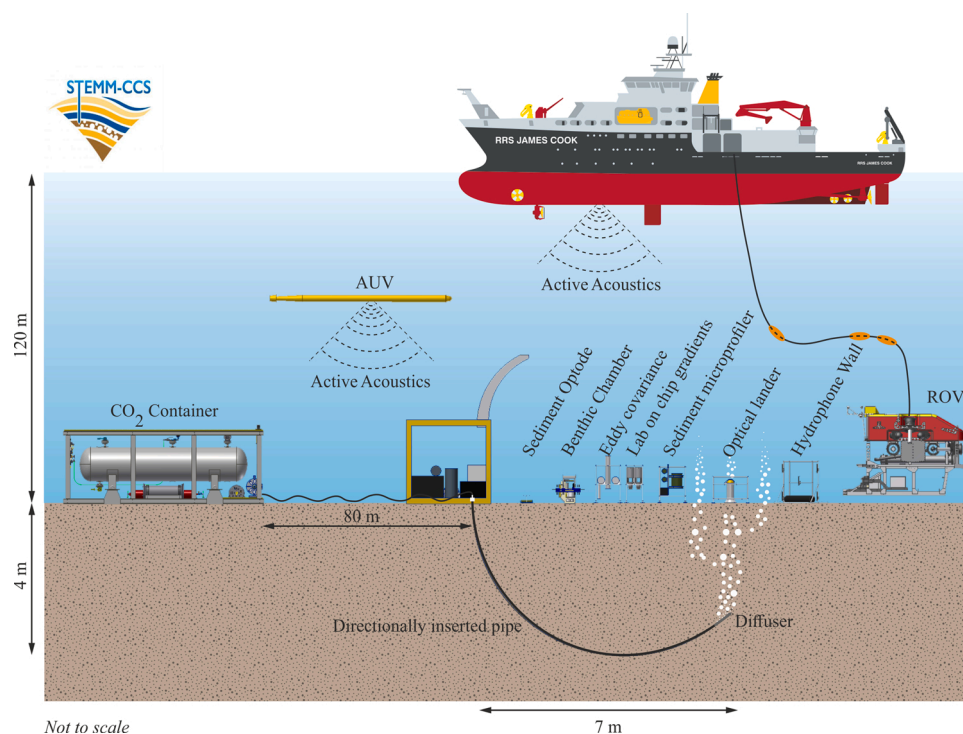


Fig. 1. Schematic overview of the CO<sub>2</sub> release experiment and a selection of deployed detection methods.



methods was used to target these different phases, i.e., the gaseous and dissolved CO<sub>2</sub> in both the sediment pore water and the overlying seawater. These methods were used to detect, characterise, and quantify the released CO<sub>2</sub>. Each method performed one or more tasks: detection of the CO<sub>2</sub> release; attribution of the release (distinguishing between CO<sub>2</sub> leaking from a reservoir and naturally emitted CO<sub>2</sub>); or quantification of the release (estimating a flux or a mass flow rate) (Table 2).

### 1.3. Experimental design and overall implementation

The CO<sub>2</sub> release experiment involved two research vessels: the UK royal research ship RRS *James Cook* (cruise number JC180; Connelly, 2019; Table 1) and the German research vessel RV *Poseidon* (cruise number POSS34; Schmidt, 2019). It was carried out near the Goldeneye platform, at 120 m water depth, in the central North Sea (Fig. 2) between 27 April and 27 May 2019. Two underwater vehicles were also used: the NOC work-class ROV (Remotely Operated Vehicle) Isis (German et al., 2003; Fig. 3a) was used to carry equipment and maneuver it on the seafloor and an AUV (Autonomous Underwater Vehicle) Gavia (Teledyne Gavia, Iceland; German et al., 2003; Fig. 3b) was used for surveying. The CO<sub>2</sub> release equipment and these vehicles were deployed from the larger vessel RRS *James Cook*.

The release experiment was designed to enable all of the detection techniques (Table 2) to be tested and their sensitivity to be quantified over a range of gas release flow rates. This was achieved by deploying as much of the seafloor-based equipment as possible around the centre of the experiment site (defined as the point on the seafloor above the end of the inserted gas injection pipe). An overview of the experiment setup is shown in Fig. 1; the relative locations of all equipment and timing of deployments are shown in Fig. 4. Most of the equipment was deployed by the ROV Isis.

For safe operation of the ROV and maneuverability at the experimental site, equipment was only deployed outside the ROV landing zone (Fig. 4). Equipment with limited battery life was recovered and redeployed by the ROV every few days over the course of the experiment, with like-for-like replacements minimising gaps in the dataset. Equipment that had to be sequentially moved in a transect across the release site (e.g., the sediment microprofiler and ROV chemical mapping surveys) was deployed on alternate nights in order to maximise the

operational ROV dive time for each survey. Whenever possible an AUV survey was conducted over the experiment site before increasing the rate of CO<sub>2</sub> release, in order to characterise any build-up or changes of gaseous CO<sub>2</sub> within the sediment. For comparison, initial AUV surveys had been conducted over the site before deploying any equipment and following the insertion of the gas release pipe. An AUV survey was also carried out after the experiment, and after all equipment was removed from the site.

The release of CO<sub>2</sub> was started at 15:19 (UTC time format used throughout the manuscript) on 11 May 2019, thus 00:00 on 11 May 2019 is considered the start of day 0 of the experiment. The gas flow rate was initially set to 6 kg/d (equivalent to the lowest achievable flow rate of 2 normal L/min; "normal" conditions are defined here as 0 °C and 1.013 bar). The CO<sub>2</sub> flow rate was sequentially increased over the duration of the experiment to a maximum of 143 kg/d (equivalent to a flow rate of 50 normal L/min) (Fig. 4), adding up to a total release of 675 kg of CO<sub>2</sub> over the course of the experiment. In most instances each flow rate was maintained for a minimum of 2 days to enable all different types of equipment to be tested under those conditions. The only exception to this was the flow rate of 14 kg/d, which was only maintained for 15 h to check that the sediments and operational setup were able to accommodate changes in CO<sub>2</sub> flow rate (i.e., that there was no abrupt release of gas from within the sediment).

When the CO<sub>2</sub> was first turned on, bubbles were observed emerging from the sediments as soon as the ROV had travelled from the CO<sub>2</sub> rig to the release site (within 30 min). At the lowest flow rate, three separate bubble streams were observed, and further bubble streams formed at higher flow rates. The dissolution of bubbles within the overlying water column was observed using the ROV. No bubbles were visible with the ROV camera at >8 m above the seabed.

The CO<sub>2</sub> injection was turned off at 11:17 on 22 May 2019, with all infrastructure recovered from the seafloor onto the RRS *James Cook* over the following 3 days. Sediment cores were taken by the RV *Poseidon* from the release site during this interval, before final ROV and AUV surveys were carried out.

## 2. Baseline site characterisation

To characterise the natural variability at the study site, the chemical,

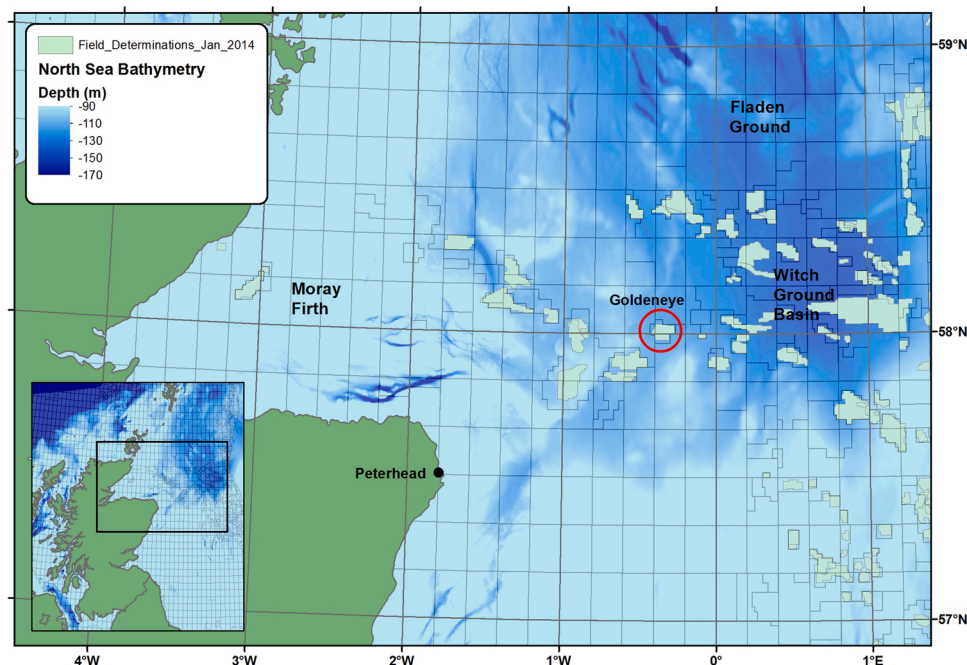


Fig. 2. Location of the Goldeneye gas field.



**Table 1**  
Research cruises for baseline and main experiments of the STEMM-CCS project.

| Vessel                    | Cruise | Date            | Purpose   | References                     |
|---------------------------|--------|-----------------|---|--------------------------------|
| RV <i>Maria S. Merian</i> | MSM63  | May 2017        | Baseline: bathymetry and subsurface imaging   | Berndt et al. (2017)           |
| RV <i>Poseidon</i>        | POS518 | October 2017    | Baseline: water chemistry, chemical and physical properties of the sediments, benthic chamber incubations (in-situ), site mapping | Linke and Haeckel (2018)       |
| RV <i>Poseidon</i>        | POS527 | August 2018     | Baseline: water chemistry, chemical and physical properties of the sediments, benthic biology, microbial activity                 | Achterberg and Esposito (2018) |
| RV <i>Maria S. Merian</i> | MSM78  | October 2018    | Baseline: bathymetry and subsurface imaging   | Karstens et al. (2019)         |
| RV <i>Poseidon</i>        | POS534 | May 2019        | CO <sub>2</sub> release experiment  | Schmidt (2019)                 |
| RRS <i>James Cook</i>     | JC180  | April- May 2019 | CO <sub>2</sub> release experiment  | Connelly (2019)                |

biological, and physical properties of the area were determined prior to the CO<sub>2</sub> release experiment (Section 1.1.3, Table 1). These baseline data were used to differentiate between the effect of the released CO<sub>2</sub> and the variability caused by natural phenomena or unrelated human activity. Customised sediment and hydrodynamic-chemical models of the Goldeneye site were developed to understand how the experimental CO<sub>2</sub> release would manifest in shallow sediments and water column.

### 2.1. Water column characteristics and chemistry

The natural dynamics of the physical and biogeochemical parameters of the water column were examined by discrete water column sampling (Section 2.1.1) and by baseline landers for continuous physical and biogeochemical measurements (Section 2.1.2).

#### 2.1.1. Discrete water sampling

Water column sampling for the characterisation of biogeochemical background conditions was conducted during POS518 (October 2017) and POS527 (August 2018) (Table 1; Achterberg and Esposito, 2018; Linke and Haeckel, 2018). Environmental baseline sampling was undertaken in an approximately 10 km by 20 km area over the Goldeneye complex with the Goldeneye platform (58° 0' 10.8" N, 0° 22' 48" W) as centre point. Water was collected using Niskin bottles located on a rosette frame equipped with a conductivity, temperature, depth (CTD) probe. Concentrations of dissolved oxygen (O<sub>2</sub>), dissolved organic and inorganic carbon (respectively, DOC and DIC), the stable carbon isotopic composition of DIC ( $\delta^{13}\text{C}_{\text{DIC}}$ ) and the oxygen isotopic composition of seawater ( $\delta^{18}\text{O}_{\text{H}_2\text{O}}$ ), pH, total alkalinity (TA), and inorganic nutrients (nitrate, phosphate and silicic acid) were established after collection and analysis by standard procedures (e.g., Murphy and Riley, 1962; Clayton and Byrne, 1993; Grasshoff et al., 1999; Dickson et al., 2007; Hansen and Koroleff, 2007; Aßmann et al., 2011). These data were compared to water column chemistry data available on the GLODAP and Cefas databases (latitude-longitude box of 56° N, 2° W to 59° N, 2° E) (GLODAP Reference Group, 2020; Cefas Data Hub, 2020) to broaden the duration and seasonal coverage of the baseline data.

To study baseline O<sub>2</sub>, nutrient and CO<sub>2</sub> fluxes across the sediment-water interface from in-situ incubations, two short-term deployments of the Biogeochemical Observatory (BIGO, Sommer et al., 2016) were conducted during cruise POS518. These incubation chamber landers are similar to the benthic chambers used during the CO<sub>2</sub> release experiment (Section 4.3.2).

#### 2.1.2. Landers for autonomous collection of in-situ data

To obtain baseline data over a longer time period and with higher temporal resolution, baseline landers equipped with autonomous in-situ sensors were deployed to gather continuous physical and biogeochemical baseline data.

A long-term seafloor baseline lander was deployed prior to the main CO<sub>2</sub> release experiment (Develogic GmbH Subsea Systems, Hamburg, Germany). It combined commercially available sensors and newly

developed technology for autonomous gathering of in-situ biogeochemical and hydrodynamic baseline data. The lander was deployed during expedition POS518 on 16 October 2017 approximately 100 m north of the actual injection site (Linke and Haeckel, 2018) at 120 m water depth. All data were logged centrally on the lander and mirrored to a number of expendable pop-up data pods. The lander was programmed to release a pod to the surface every 3 months to relay collected data via Iridium satellite. The pop-up system did not work well but the lander was recovered during expedition JC180 in May 2019 and several months of data were found to have been recorded for the majority of the sensors.

As it was not possible to recover the Develogic long-term lander before the release experiment, additional landers for experimental background measurements were prepared by NOC and GEOMAR Helmholtz Centre for Ocean Research Kiel and were deployed for the duration of the release experiment. The landers were positioned approximately 350 m southeast and northeast of the experiment site respectively (see Fig. 4), sufficiently far to provide unperturbed background data. These landers provided measurements of physical (temperature, salinity and water currents) and biogeochemical (O<sub>2</sub>, carbonate chemistry and nutrients) parameters of the bottom part of the water column, with some parameters measured at high resolution (up to 0.1 Hz). With automated data collection, the three observational systems were able to provide a sound characterisation of the marine environment at the experiment site.

### 2.2. Baseline environmental study

The environmental baseline was assessed to establish conditions prior to the experimental work, to distinguish environmental impacts as a result of CO<sub>2</sub> storage from those produced by other factors. To this end, the sediment and pore water characteristics were determined (Section 2.2.1), the benthic community was characterised (Section 2.2.2), and the area was mapped (Sections 2.2.3 and 2.2.4) prior to the controlled CO<sub>2</sub> release experiment.

#### 2.2.1. Sediment coring

To understand the effects of CO<sub>2</sub> injection on sediment geochemistry, baseline values for relevant parameters, as well as their spatio-temporal variability, were determined. Baseline data were collected during the baseline cruises POS518 and POS527 to the study site (Linke and Haeckel, 2018; Achterberg and Esposito, 2018) (Table 1).

Sediment cores were obtained using push, gravity and multi corers and sub-sampled for biogeochemical analyses of the pore waters (nutrients, cations, anions, TA, DIC,  $\delta^{13}\text{C}_{\text{DIC}}$ ,  $\delta^{18}\text{O}_{\text{H}_2\text{O}}$ ) and the solid phase (porosity, particle size, TOC, TON,  $\delta^{13}\text{C}$  of organic and inorganic carbon, chemical composition).

#### 2.2.2. Benthic biology

Benthic organisms living on or in sediments can affect the sediment structure and biogeochemical processes locally as well as over larger

**Table 2**

Summary of targeted phases, techniques and objectives of the release experiment for the detection and/or attribution and/or quantification of the released CO<sub>2</sub>.

| Measurement target                            | Technique / method                          | Objective (section in paper)   | Detection (D), Attribution (A), Quantification (Q)<br>*               |
|---|---|--|---|
| Seafloor and sub-seafloor                     | Benthic biological imaging                  | Automated image collection and annotation for baseline and identification of CO <sub>2</sub> -related changes in seafloor biota (Section 2.2.2)                                | D   |
|   |   | Collection and chemical analysis of sediments and pore water around bubble streams (Section 4.1.1)   | DA  |
|   | Sediment coring                             | In-situ profiles of temperature, pH, oxygen, and other parameters in the sediments (Section 4.1.2)   | D   |
|   | Sediment microprofiler                      | pH and temperature measurement within the sediment pore water (Section 4.1.3)  | D   |
|   | Sediment optodes                            | Measuring physical structure of seafloor and imaging of potential gas pockets (Section 4.1.4)  | DQ  |
|   | AUV Chirp Profiler                          | Direct optical measurement of bubble size and gas flow rate of a bubble stream (Section 4.2.1)   | Q   |
|   | Bubble imaging                              | Direct measurement of gas flow rate of a bubble stream (Section 4.2.2)   | Q   |
|   | Funnel capture of gas bubbles               | Collection of gas bubbles from a bubble stream for tracer analysis (Section 4.2.2)   | DAQ   |
|   | Gas sampling                                | Direct acoustic measurements of bubble size and gas flow rate (Section 4.2.3)  | DQ  |
|   | Gaseous CO <sub>2</sub> in the water column | Passive acoustics  | Location of bubble stream sites from the ship and AUV (Section 4.2.4) |
| Multibeam and sidescan acoustics              |   | Optical observation of bubble streams and measurement of dissolved CO <sub>2</sub> and related seawater parameters by using a towed and video-guided CTD probe (Section 4.3.1) | D   |
| Video-CTD imaging                             |   | Chemical analysis of sampled water (Section 4.3.1)   | DA  |
| Dissolved CO <sub>2</sub> in the water column | Niskin bottle sampling                      | Pumping of seawater in the vicinity of bubble streams directly to the ship for   | DAQ   |

**Table 2 (continued)**

| Measurement target | Technique / method             | Objective (section in paper)  | Detection (D), Attribution (A), Quantification (Q)<br>* |
|--------------------|--------------------------------|---|---|
|                    | Benthic chambers               | chemical analysis (Section 4.3.1)   |   |
|                    |                                | Benthic fluxes of DIC, total oxygen uptake, nutrients, and other parameters (Section 4.3.2)   | DAQ   |
|                    | Eddy covariance                | Quantify vertical flux and total DIC content seawater in the vicinity of bubble streams with point measurements of current and pH (Section 4.3.3) | DAQ   |
|                    |                                | Quantify vertical flux and total DIC content of seawater in the vicinity of bubble streams with lab-on-chip sensors (Section 4.3.4)               | DAQ   |
|                    | Chemical gradient measurements | Mapping spatial extent and DIC content of seawater in the vicinity of bubble streams with real-time data (Section 4.3.5)                          | DA  |
|                    |                                | Mapping spatial extent and DIC content of seawater in the vicinity of bubble streams (Section 4.3.6)  | D   |

\* Note the categorisation (D, A, Q) is specific to this study and does not preclude use of the method in other ways. Shaded cells represent methods/analyses performed in-situ, and unshaded cells represent methods that relied on sample collection and subsequent analysis on board the ship or onshore.

areas (Van Hoey et al., 2008; Montserrat et al., 2009). Additionally, the release of CO<sub>2</sub> may affect the benthic fauna near or at a release site.

Sampling for benthic macrofauna (body size 0.5–10 mm) of the Goldeneye area was carried out in August 2018 during the RV *Poseidon* cruise POS527 using a winch operated box-corer (50 cm width × 50 cm depth) (Achterberg and Esposito, 2018). A total of 76 samples were collected from 75 sites selected according to sediment type, fishing pressure and pockmark location. All fauna were sorted and identified to the lowest possible taxonomic level under a stereomicroscope, with individuals and species abundances per sample recorded. Identification and quantification of interactive effects of sediment type, fishing pressure and distance from pockmark on community abundance and diversity measures were determined.

Benthic megafauna (>10 mm; sensu Grassle et al., 1975) at the experimental site were assessed using seabed photography before the experiment started. Photographic surveys were conducted with the Gavia AUV during the JC180 cruise; one survey was conducted at the experimental site and another at a site distant from it. Seabed photographs were captured using a GRAS-14S5M-C camera with a Tamron TAM 23FM08-L lens mounted to the AUV (Connelly, 2019). The camera captured photographs at a temporal frequency of 1.875 frames per second, a resolution of 1280 × 960 pixels, from a target altitude of 2 m above the seafloor. The total seafloor area represented, and the extent of overlap between photographs, were estimated using the camera specifications, location and altitude of the camera, and any overlapping photographs were removed from the analysis. The photographic

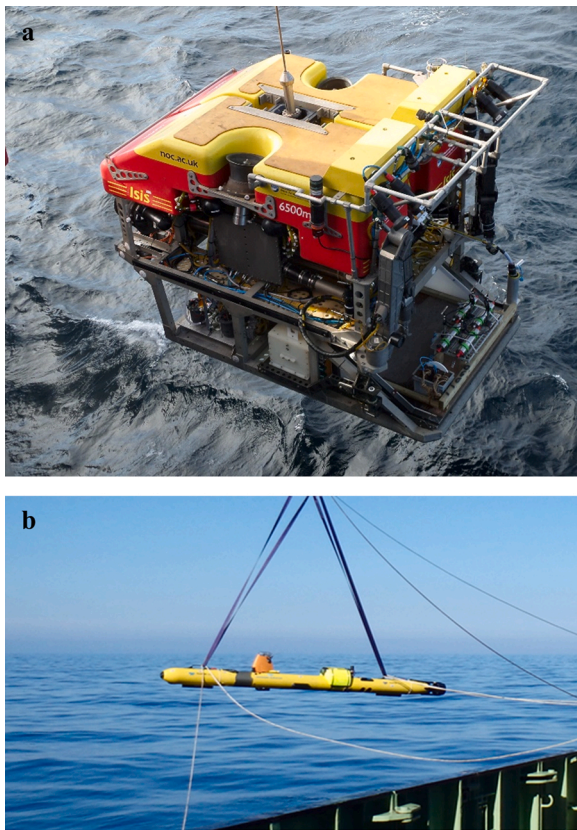


**Fig. 3.** Underwater vehicles deployed during the field experiment. (a) The work-class remotely-operated vehicle Isis, which was used to deploy most of the seafloor-based equipment during the STEMM-CCS release experiment. (b) The Gavia autonomous underwater vehicle, which performed seismic, bathymetry, imaging, sidescan, and chemical surveys.

datasets used for analysis were comprised of 446 images representing 1053 m<sup>2</sup> of seabed from the experimental area, and 981 images representing 2366 m<sup>2</sup> seabed from the distant site. Megafaunal specimens were enumerated and classified to morphotypes using the BIIGLE 2.0 annotation software (Langenkämper et al., 2017) through a combination of manual annotation and implementation of the MAIA unsupervised machine learning algorithm (Zurowietz et al., 2018). Megafaunal density, diversity and community composition were calculated for the test site, and compared with those from the distant site.

### 2.2.3. Site mapping

The baseline mapping work for the Goldeneye site comprised three related phases, covering different extents and levels of detail as proposed by Widdicombe et al. (2018). Phase 1 collated existing industry and public data to establish a broad overview of the study area and to identify data gaps requiring survey effort. This analysis pointed to sediment type as the main habitat driver for the area; however, no detailed, full-coverage maps of this parameter existed for the Goldeneye site. Phase 2 combined the existing data with spatial statistical modelling techniques (Random Forest, Generalised Additive Models) to predict the distribution of sediment type and the density of a key crustacean benthic species, *Nephrops norvegicus*, across the experiment site. In addition, shipboard multibeam bathymetry data were collected during three expeditions at sea, mapping the seafloor to a 10 × 10 m or 5 × 5 m resolution (Berndt, 2017; Achterberg and Esposito, 2018; Connelly, 2019). Phase 3 involved dedicated data collection at even finer resolution (as described as “Tier 4” in Widdicombe et al., 2018) to characterise fine-scale bathymetric variability at the Goldeneye site, and to monitor the experimental site before, during and after the controlled release

experiment (during cruise JC180). These activities included the acquisition of high-resolution (0.25 × 0.25 m) bathymetry and sidescan sonar, photographic, and environmental data with the Gavia AUV, and photogrammetry data collected by the ROV Isis (Connelly, 2019).

### 2.2.4. Anthropogenic activities

The two most significant impacts of anthropogenic activities visible at the seafloor around the Goldeneye site are from ceased oil and gas (O&G) extraction (and its associated structures) and commercial fishing activity. All anthropogenic structures, such as the oil and gas infrastructure, were mapped within the project GIS, based on data from O&G infrastructure databases (UKOilandGasData, 2007; <http://www.ukoilandgasdata.com/>). The feature locations were buffered according to the physical dimensions of the structures (e.g., pipe diameters and typical well dimensions) and by typical near-field modifications (e.g., scour pits, etc.) using standard buffer values to visualise actual footprints. The Goldeneye platform was also included and buffered to account for the potential for historical contamination according to literature values for persistent contaminants. Field studies in the North Sea have demonstrated that the effects of dumping of cuttings (physical smothering, organic enrichment and chemical contamination) are persistent and principally confined to benthic communities within a 1–2 km radius of platform sites (see Breuer et al., 2004 and references therein; Gates and Jones, 2012; Jones et al., 2012). Vessel Monitoring System layers for 2007–2015 (vessels over 15 m), sourced from the UK Marine Management Organisation (data obtained from the MMO via: <https://data.gov.uk/>; accessed January 2019), were used to represent the intensity of fishing effort across the site. Trawl scar densities were estimated from the Gavia AUV Geoswath surveys and used as a proxy for the cumulative pressures in specific areas.

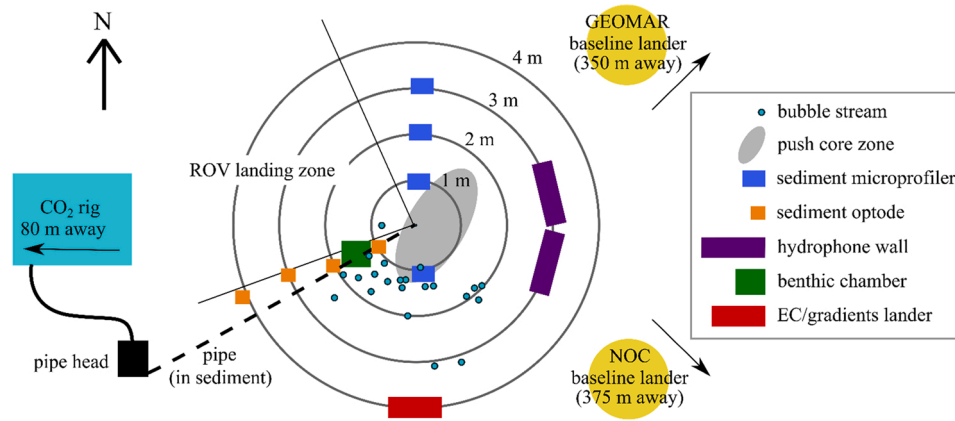
### 2.3. Modelling to inform experimental design and predict impact

In order to understand, a priori, how the experimental CO<sub>2</sub> release would manifest in shallow sediments and the water column, customised sediment and hydrodynamic-chemical models of the Goldeneye site were developed. These models had high spatial and temporal resolution to resolve chemical changes at the centimeter to meter scale (in sediments) and meter to kilometer scale (in water column). Models of sediment chemistry were used to estimate the change in solute concentrations, including DIC and O<sub>2</sub>, due to redox processes in the top 30 cm of the sediments (Dale et al., 2015). Models of two-phase geophysical flow were used to estimate the degree of CO<sub>2</sub> retention, flow pathways in the sediments, and the mode of exchange between sediments and the water column using modified Navier-Stokes-Darcy equations. These estimates can predict the footprint of CO<sub>2</sub> release at the seabed, the gas breakthrough time, but most vitally, the required injection rate for sustained gas breakthrough to the water column.

This abundance of data was then exploited in models of multi-scale hydrodynamic transport in the water column, including multi-phase bubble stream dynamics (Alendal and Drange, 2001; Dewar et al., 2015; Gros et al., 2019) linked to local and regional General Circulation Models coupled to a model of carbonate chemistry (Artoli et al., 2012). These models simulated the transport and dispersion of CO<sub>2</sub> in the water column and the resulting chemical changes detectable by sensors (Cazenave et al., 2018). These estimates of the physio-chemical footprints of the released CO<sub>2</sub> enabled informed planning of the observational layout and the choice of sensors and parameters measured from fixed and moving platforms (Hvidevold et al., 2015; Greenwood et al., 2015; Hvidevold et al., 2016; Alendal, 2017; Oleynik et al., 2020). These predictions also estimated the footprint of increased acidification (Blackford et al., 2020), assisting in environmental impact assessments.

Medium resolution models (Blackford et al., 2017) were used to spatially and temporally extrapolate our knowledge of natural variability as a key question was: can we distinguish potentially small signals of a CO<sub>2</sub> release from the complex natural variability in the marine





|  |                               | Date in May 2019  | 7  | 8  | 9  | 10 | 11 | 12 | 13 | 14 | 15 | 16 | 17 | 18 | 19 | 20 | 21 | 22 | 23 | 24 | 25 | 26 | 27 |  |
|--|-------------------------------|-------------------|----|----|----|----|----|----|----|----|----|----|----|----|----|----|----|----|----|----|----|----|----|--|
|  |                               | Day of experiment | -4 | -3 | -2 | -1 | 0  | 1  | 2  | 3  | 4  | 5  | 6  | 7  | 8  | 9  | 10 | 11 | 12 | 13 | 14 | 15 | 16 |  |
| Ships, vehicles, and CO <sub>2</sub> rig | RRS <i>James Cook</i> on site |                   |    |    |    |    |    |    |    |    |    |    |    |    |    |    |    |    |    |    |    |    |    |  |
|  | RV <i>Poseidon</i> on site    |                   |    |    |    |    |    |    |    |    |    |    |    |    |    |    |    |    |    |    |    |    |    |  |
|  | Gas rig in water              |                   |    |    |    |    |    |    |    |    |    |    |    |    |    |    |    |    |    |    |    |    |    |  |
|  | Gas turned on                 |                   |    |    |    |    |    |    |    |    |    |    |    |    |    |    |    |    |    |    |    |    |    |  |
|  | AUV surveys                   |                   |    |    |    |    |    |    |    |    |    |    |    |    |    |    |    |    |    |    |    |    |    |  |
| Sampling equipment                       | NOC baseline lander           |                   |    |    |    |    |    |    |    |    |    |    |    |    |    |    |    |    |    |    |    |    |    |  |
|  | GEOMAR baseline lander        |                   |    |    |    |    |    |    |    |    |    |    |    |    |    |    |    |    |    |    |    |    |    |  |
|  | Sediment cores (push)         |                   |    |    |    |    |    |    |    |    |    |    |    |    |    |    |    |    |    |    |    |    |    |  |
|  | Sediment cores (gravity)      |                   |    |    |    |    |    |    |    |    |    |    |    |    |    |    |    |    |    |    |    |    |    |  |
|  | Sediment microprofiler        |                   |    |    |    |    |    |    |    |    |    |    |    |    |    |    |    |    |    |    |    |    |    |  |
|  | Sediment optodes              |                   |    |    |    |    |    |    |    |    |    |    |    |    |    |    |    |    |    |    |    |    |    |  |
|  | Gas bubble imaging            |                   |    |    |    |    |    |    |    |    |    |    |    |    |    |    |    |    |    |    |    |    |    |  |
|  | Gas bubble sampling           |                   |    |    |    |    |    |    |    |    |    |    |    |    |    |    |    |    |    |    |    |    |    |  |
|  | Hydrophone walls              |                   |    |    |    |    |    |    |    |    |    |    |    |    |    |    |    |    |    |    |    |    |    |  |
|  | Water sampling (ROV bottles)  |                   |    |    |    |    |    |    |    |    |    |    |    |    |    |    |    |    |    |    |    |    |    |  |
|  | Water sampling (video CTD)    |                   |    |    |    |    |    |    |    |    |    |    |    |    |    |    |    |    |    |    |    |    |    |  |
|  | Benthic chambers              |                   |    |    |    |    |    |    |    |    |    |    |    |    |    |    |    |    |    |    |    |    |    |  |
|  | Eddy covariance               |                   |    |    |    |    |    |    |    |    |    |    |    |    |    |    |    |    |    |    |    |    |    |  |
|  | Chemical gradients            |                   |    |    |    |    |    |    |    |    |    |    |    |    |    |    |    |    |    |    |    |    |    |  |
|  | Chemical mapping with ROV     |                   |    |    |    |    |    |    |    |    |    |    |    |    |    |    |    |    |    |    |    |    |    |  |
| Gas flow rate                            | 143 kg/day                    |                   |    |    |    |    |    |    |    |    |    |    |    |    |    |    |    |    |    |    |    |    |    |  |
|  | 86 kg/day                     |                   |    |    |    |    |    |    |    |    |    |    |    |    |    |    |    |    |    |    |    |    |    |  |
|  | 29 kg/day                     |                   |    |    |    |    |    |    |    |    |    |    |    |    |    |    |    |    |    |    |    |    |    |  |
|  | 14 kg/day                     |                   |    |    |    |    |    |    |    |    |    |    |    |    |    |    |    |    |    |    |    |    |    |  |
|  | 6 kg/day                      |                   |    |    |    |    |    |    |    |    |    |    |    |    |    |    |    |    |    |    |    |    |    |  |

Fig. 4. STEMM-CCS experimental geometry and timeline. (Top) Schematic overview of representative positions of all deployed equipment around the experimental site. All observed bubble streams are indicated on the map although not all were active simultaneously. Equipment sizes are approximately to scale. (Bottom) Timing of the ships, vehicles, deployed equipment, sampling, and CO<sub>2</sub> injection flow rates after the initial setup phase of the experiment.

system? The baseline and release experiment data were used to evaluate the performance of the various models, to assess their utility as useful tools for studies of impact and monitoring strategy, and to assess other methods for analysing data streams to detect leakage, such as the stoichiometric C<sub>seep</sub> method (Botnen et al., 2015).

### 3. CO<sub>2</sub> release equipment

A fundamental objective of the field experiment was to release gas from a point within the sediments approximately 3 m below the seafloor surface. To do this, the gas needed to be released from tanks positioned directly on the seabed, with no connection to the surface, to allow safe ROV operations and to increase ship mobility. A central design consideration was the ability to change the injection flow rates during the field experiment to simulate different leakage rate scenarios. Consequently, it was necessary to insert a gas release pipe on site (Section 3.1) and to

connect it to a gas storage and delivery system (Section 3.2) that was custom-built for the STEMM-CCS field experiment.

#### 3.1. Pipe insertion setup

The injection of gas into shallow sediments in the North Sea at 100 km offshore from Scotland presented a major engineering challenge. Directional drilling from land, as done in the QICS project (Taylor et al., 2015), was not an option. The solution was to draw on well-known cone penetrometer techniques, whereby an instrumented rod is pushed vertically downwards into the seabed using a subsea drive unit. This technique was adapted to push a pre-curved steel pipe downwards into the seabed such that the end of the pipe was located 3 m below the seabed with an upward attitude (Fig. 5a). The upward attitude of the outlet was necessary to prevent the gas from tracking back along the outside of the pipe rather than finding a natural pathway up through the

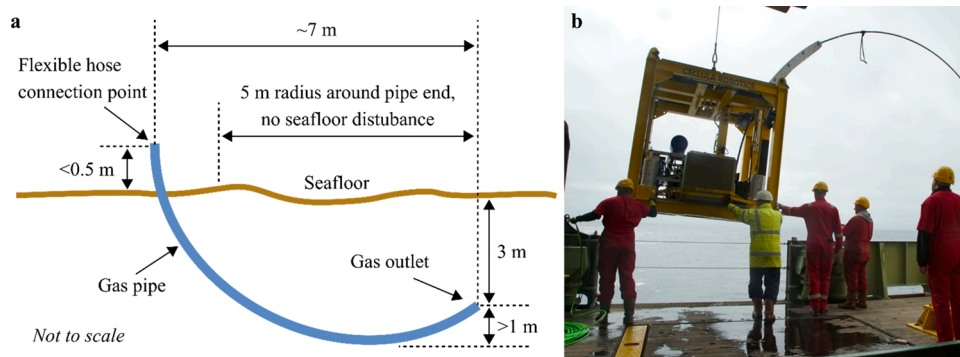


Fig. 5. Gas release pipe. (a) Schematic of gas release pipe geometry. (b) Pipe insertion rig and pipe being deployed from RRS *James Cook*.

sediment. The design and manufacture of the pipe insertion rig was contracted to Cellula Robotics (Cellula Robotics Ltd., Burnaby, Canada), following an open tender exercise.

The pipe insertion rig (Fig. 5b) was a 2.3 m cubic steel frame. It housed a hydraulic power pack to drive a set of clamp rollers that firmly held the pipe and slowly rotated to drive the pipe along its own axis into the sediment. Control and electrical power to the hydraulic unit was provided via an umbilical cable from the ship. The umbilical also carried live video back to the ship (i) to verify the rig had landed on a suitable site, (ii) to confirm the orientation of the rig (and hence the direction that the pipe would be inserted), and (iii) to monitor progress of the pipe as it was pushed into the sediment. The rig had sufficient push force to jack up its 6 t mass should the pipe encounter an impenetrable object. An inclinometer was included to provide early warning of any change of frame angle that would result from such an occurrence.

The carbon steel pipe (9 m length, 38.1 mm outer diameter, 12.7 mm inner diameter) was pre-curved to a radius of 6.9 m. A retractable 'goose-neck' was included to support the pipe during deployment. The outlet end of the pipe was closed with a pointed tip to aid penetration through the sediment. Just behind the tip were a number of 12.7 mm diameter gas exit holes drilled through the pipe wall at a 45° backward slant to prevent them becoming clogged with sediment. Inside the drilled portion of the pipe was a 460 mm long sintered stainless-steel diffuser with a pore size of 9  $\mu\text{m}$  to ensure the gas flow was distributed evenly across the outlet holes. The pipe inlet, which remained above the seabed, had a quick-connect fitting for connection to the gas supply via a flexible hose.

### 3.2. Gas release system

It was originally intended that the gases would be supplied in standard industrial cylinders and delivered to the seabed on pallets. However, commercially available cylinders are not designed for a subsea environment and establishing leak-proof connections between the pallets would have been problematic. It was therefore necessary to design and build a custom gas storage system.

A pair of custom-made bulk CO<sub>2</sub> storage tanks, connected to act as one single storage volume of 5.6 m<sup>3</sup>, was procured from City Gas (City Gas EOOD, Stara Zagora, Bulgaria). This storage volume was sufficient to accommodate 3 t of liquid CO<sub>2</sub> with a 1.7 m<sup>3</sup> vapour headspace at 20 °C. It is usual for bulk CO<sub>2</sub> to be stored cryogenically to reduce storage pressure to around 20 bar. However, this requires insulated tanks and a cooling plant to maintain the temperature at around -20 °C, which was not viable in a marine setting. The tanks were therefore uninsulated and designed for a maximum working pressure of 80 bar. This was sufficient to allow for an ambient temperature in excess of 30 °C, which was unlikely to be encountered during springtime in the UK. At the seabed, the ambient temperature would be around 8 °C, resulting in a storage pressure of 42 bar(a) (absolute pressure). The bulk storage tanks, along with the other equipment described below, were mounted in a steel

deployment frame (5.5 m length, 2.55 m width, 2 m height) (Fig. 6) that had a gross weight of 13 t (including a total of 3.3 t of liquid CO<sub>2</sub>).

The gas rig also housed 200 L of a tracer gas mixture (BOC, UK) comprised of molar fractions of 58.98 % krypton (Kr), 1.77 % sulfur hexafluoride (SF<sub>6</sub>) and 0.11 % octafluoropropane (C<sub>3</sub>F<sub>8</sub>), with the balance consisting of gaseous CO<sub>2</sub> (Section 4.2.2). The tracer gas mixture was decanted into four manifolded bladder accumulators (QHP, England) for deployment. The accumulators were kept charged to a constant pressure of 30 bar(a) via a regulated gas feed from the bulk CO<sub>2</sub> tanks. This was necessary to aid stability of flow and to ensure that nearly all of the mixture could be extracted when submerged at 120 m water depth with an external pressure of approximately 12 bar. The tracer gas mixture was fed into a custom-designed control unit (Fig. 7) where the flow was regulated through a mass flow controller (MFC) (Bronkhorst, UK) and then mixed into the main CO<sub>2</sub> line. The mixed gas line then re-entered the control unit where a second MFC metered the overall flow rate. The MFCs worked as a master-slave pair whereby the mixed gas flow was user-controlled and the tracer gas mixture flow maintained a pre-set mass ratio. For the experiment the ratio was set at



Fig. 6. Deployment of the gas storage and release system.

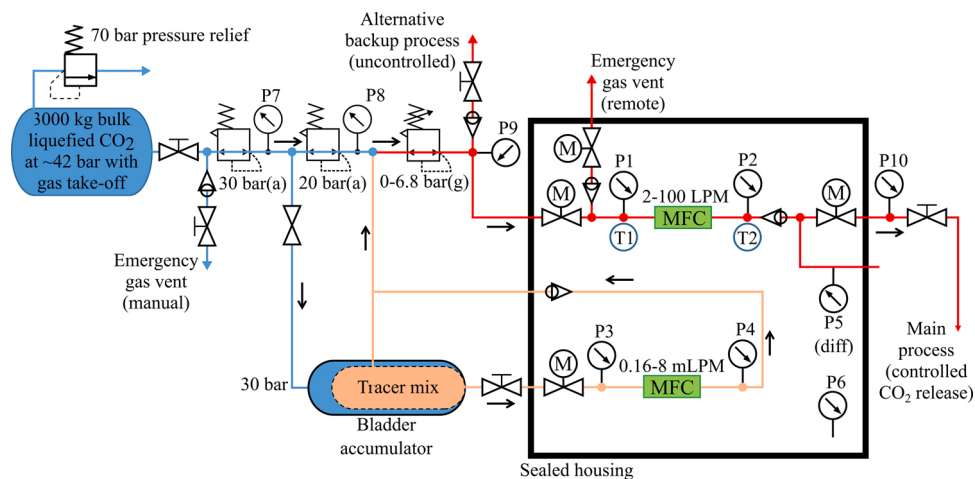


Fig. 7. Schematic of the gas control unit.

10,000:1 to yield molar fractions of 58.98 ppm Kr, 1.77 ppm SF<sub>6</sub> and 0.11 ppm C<sub>3</sub>F<sub>8</sub> in the final injection gas. This target ratio was kept constant throughout the release experiment.

The overall flow rate was adjustable from 0 to 100 normal litres per minute which is equivalent to a mass flow range of 0–285 kg/d. Remote adjustment of the MFCs and feedback of engineering data for flow rate, pressure and temperature were achieved using an optical modem that enabled communication to the research ship via the ROV's umbilical cable. The control unit was powered by a pair of 24 V lead-acid batteries housed in stainless steel cylinders. From the control unit the mixed gas flowed to a valve panel where an outlet could be selected. These outlets included a sample port from which 'raw' samples could be collected to verify the composition of the gas mixture, a 100 m long flexible hose that was connected by ROV to the buried gas pipe, and a second 'emergency' flexible hose that could be laid on the seabed to release gas directly into the water column should the buried pipe be blocked and not allow gas to flow.

After the successful insertion of the curved pipe and deployment of the CO<sub>2</sub> storage rig, the ROV carried the 100 m long hose from the CO<sub>2</sub> rig to the pipe inlet. The ROV's manipulator arm was used to connect the hose to the pipe inlet. The gas was turned on using an optical modem connection between the ROV and the CO<sub>2</sub> rig.

#### 4. CO<sub>2</sub> detection techniques and methodologies

During the controlled CO<sub>2</sub> release experiment diverse techniques and methods were employed to detect and/or quantify the CO<sub>2</sub> in the sediments (Section 4.1) and the water column (Sections 4.2 and 4.3).

##### 4.1. Detection of gaseous and dissolved CO<sub>2</sub> in the sediments

A variety of measurements were undertaken to characterise the seafloor and quantify the CO<sub>2</sub> remaining below the seafloor in gaseous or dissolved form. Sediment cores were collected for biogeochemical analyses of the pore waters and the sediments themselves (Section 4.1.1). In-situ measurements of electrochemically measurable parameters were made using a microprofiler setup (Section 4.1.2) and pH optodes (Section 4.1.3) to determine signatures of the CO<sub>2</sub> in the sediments. Seismic profiling using an AUV aimed to image and characterise the underlying subsurface sediments and to identify any changes that may occur as a result of the gas release (e.g., the formation of gas pockets) (Section 4.1.4).

##### 4.1.1. Sediment coring

Analyses of the geochemistry of the sediments and their pore waters, as well as the sediment's physical properties, are useful for detecting and

locating a sub-seafloor CO<sub>2</sub> source and for quantifying the rate of reactions that occur in the sediments. Gaseous CO<sub>2</sub> migrating through sediments will dissolve in the pore water and will react with the sediment's mineral phases such as carbonates and silicates. Thus, sediment cores were examined for parameters indicative of CO<sub>2</sub> dissolution, mineral dissolution, and changes in the physical properties and composition of the sediment.

Three different types of sediment cores were collected during different phases of the CO<sub>2</sub> release experiment: push cores, gravity cores, and multicores. Push cores (up to 30 cm length) were retrieved prior, during, and after the CO<sub>2</sub> release experiment using the ROV manipulator arm. The advantage of this core sampling strategy is that the core locations can be targeted on a cm scale, e.g., close to bubble streams or pockmarks. Up to six push cores were taken on selected dives at each stage of the CO<sub>2</sub> release experiment (see indicative locations on Fig. 4 and photo in Fig. 8a). The sandy nature of the sediment meant that the holes caused by the coring were rapidly infilled to only leave a shallow indent on the seafloor surface that quickly disappeared. After recovery the push cores were processed on board the ship (RRS *James Cook*) in a chamber filled with nitrogen gas to minimise contact with oxygen within a controlled temperature lab set to the seabed temperature (~8 °C). Gravity cores were also taken from the RV *Poseidon* to investigate deeper layers of the sediments (up to 4.5 m below seabed) as well as multicores (up to 60 cm below the seabed) taken at similar locations, which enabled sampling of the sediment-water interface. The gravity and multicores were obtained after the CO<sub>2</sub> injection had stopped and all the equipment had been recovered (Fig. 4) to ensure the integrity of the sediments was maintained during CO<sub>2</sub> release. The gravity cores and multicores were processed under ambient conditions on board the RV *Poseidon*. All cores were sub-sampled for biogeochemical analyses of the pore waters (nutrients, cations, anions, TA, DIC, δ<sup>13</sup>C<sub>DIC</sub> and δ<sup>18</sup>O<sub>H2O</sub>) and the sediments (geochemistry, mineralogy, total carbon and nitrogen content, total organic carbon, δ<sup>13</sup>C of organic carbon, particle size and porosity) (Connolly, 2019; Schmidt, 2019).

##### 4.1.2. Sediment microprofiler

In-situ sampling and analysis of pore water has significant advantages over core sampling and ex-situ pore water extraction because concentrations of many chemical species may change during sampling or cannot be sampled accurately as they have steep vertical gradients near the sediment-water interface (Revsbech and Jørgensen, 1986; de Beer, 2000; Kühl and Revsbech, 2001; Gieseke and de Beer, 2004). In-situ analyses of sediment pore waters can be achieved using micro-sensors: miniaturised electrochemical or optical sensors.

The sediment microprofiler was equipped with several microsensors (Fig. 8b and c) that measure the concentrations of different chemical



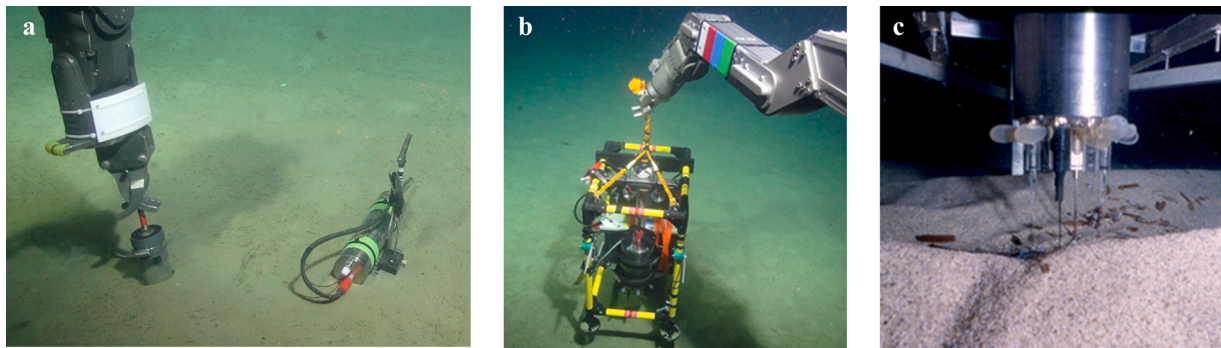


**Fig. 8.** Selection of methods employed to detect dissolved  $\text{CO}_2$  in the sediment. (a) The ROV arm taking a push core (left) next to a sediment optode (right). (b) Sediment microprofiler being deployed by the ROV. (c) Microprofiler making a profile measurement (at an unrelated site, for illustration of the equipment). The microsensors are partially inserted into the sediments and the pressure compensating balloons are visible.

species using electrochemical techniques. As the tip diameter is  $<50\ \mu\text{m}$ , the microsensors impose minimal disturbance to the sediments and provide high resolution vertical profiles of  $\text{O}_2$ , pH, hydrogen sulphide ( $\text{H}_2\text{S}$ ), redox state, and temperature within the sediment. The microprofiler can be deployed for up to 72 h at  $2\ ^\circ\text{C}$ . The sensors were calibrated on the ship, before and after each deployment.

The microprofiler was deployed along transects from outside the bubble stream area towards the experiment epicentre. It was positioned on the seafloor by the ROV (Fig. 8b), and the profiling was switched on by activating a magnetic switch with the ROV manipulator arm. The device was programmed to make measurements at  $250\ \mu\text{m}$  intervals downwards through the sediments. Measurements began a few cm above the seabed and extended to 12 cm depth into the sediment. Each profile took approximately 50 min to record. The  $\text{O}_2$  profiles were used to calculate vertical  $\text{O}_2$  fluxes using Fick's law of diffusion (Jørgensen and Revsbech, 1985).

#### 4.1.3. Sediment optodes

Four stand-alone optical sensors (optodes) continuously monitored the pH in the sediment pore waters at 20 cm depth. They were placed at distances of 1, 1.4, 4 and 7 m away from the bubble streams and recorded pH prior to, during and after the  $\text{CO}_2$  release (Fig. 8a).

The optodes utilised the pH-dependent fluorescence of an indicator dye immobilised into a proton-permeable polymeric matrix (hydrogel). An additional material with pH-independent fluorescent properties provided a reference measurement (Klimant et al., 2001). Trials of an earlier version of the system (Staudinger et al., 2019) showed that the response of the optodes was very slow at Goldeneye, so a new optode system that utilised polymeric microparticles was deployed and this substantially improved the optode response time. The sediment optodes used commercially available opto-electronics from PyroScience (FireStingO2), a custom-built logger unit (Max Planck Institute for Marine Microbiology, Bremen, Germany) and rechargeable batteries, all placed in a titanium housing. An optical fibre guided the light between the logger and the pH-sensing element. The distal end of the fibre housed the sensing material and was enclosed in a stainless-steel sleeve for rigidity in the sediment. The temperature was recorded by a PT100 sensor. The temperature was needed to calculate the pH accurately and incidentally demonstrated that reactions between the sediments and  $\text{CO}_2$  generated heat.

For the deployment, the sediment optode loggers were mounted on a perforated metal sheet with an ROV handle attached on top and the pH and temperature probes extending 20 cm below the sheet. Prior to the deployment the pH sensors were calibrated and set to measure every 5 s for 1 min, then to sleep for 15 min. The four sediment optode loggers were deployed by the ROV four days before the  $\text{CO}_2$  release was initiated. They were left in place throughout the experiment and recovered shortly after the  $\text{CO}_2$  release stopped (Fig. 4).

#### 4.1.4. AUV-mounted chirp sub-bottom profiling

An AUV-mounted chirp sub-bottom profiler was used to image the subsurface in and around the release site. This sonar-based system is sensitive to density and velocity changes in the sediments, which permits imaging of sediment stratification and to identify and characterise gas pockets in the seafloor. Data were collected in a dense grid centred above the  $\text{CO}_2$  release point with a line spacing of between 2 and 5 m from elevations of 7.5 and 2 m above the seabed. The chirp sonar used a digitally produced 14–21 kHz acoustic transmission and matched filter processing to achieve both high resolution and good penetration of soft sediments up to 10 m below the seabed. Surveys were carried out before the gas release began, during the release at rates of 6, 29, and 143 kg/d, and after the release was stopped to observe the migration of  $\text{CO}_2$  within the sediments and any lasting effects it may have had.

#### 4.2. Detection of gaseous $\text{CO}_2$ in the water column

A range of custom developed equipment was deployed to detect, characterise, and quantify the  $\text{CO}_2$  gas bubbles in the water column. Physical bubble characteristics were measured with optical and acoustic methods (Sections 4.2.1, 4.2.3 and 4.2.4). Gas chemistry was analysed from collected gas samples and physical measurements of flow rates were made using funnel-based methods (Sections 4.2.1 and 4.2.2).

##### 4.2.1. Gas bubble imaging (Optical Lander)

An Optical Lander was custom-built to obtain optical and physical measurements of the gas flow rate into the water column. The design for the optical measurements incorporated two underwater cameras (Sony FDR-X3000 Action Cam) in custom housings opposite an illuminated scale board. The frame was placed directly over an individual seep by the ROV, such that the bubble stream passed directly between the cameras and the screen. The visible scale on the screen enabled the gas flow to be quantitatively estimated by using the camera footage to measure the size of each bubble passing in a given time period and then estimating the total volume of gas observed. The frame was deployed successfully for one measurement period, collecting 15 min of useable footage at 90 frames per second before being recovered. An alternative mechanical measurement of the flow rate of an individual seep was accomplished using an “inverted rain gauge”, which was placed over the centre of the Optical Lander, roughly 0.5 m above the seabed (Fig. 9b). This gauge collected gas from the underlying seep until a known volume of gas was collected, at which point it tilted upwards emptying the gas and resetting itself. By observing how often the gauge tilted, a measurement of gas flow rate could be made.

##### 4.2.2. Gas bubble sampling

In monitoring for potential leakage from an offshore  $\text{CO}_2$  storage site, it is important to be able to demonstrate that an observed anomaly

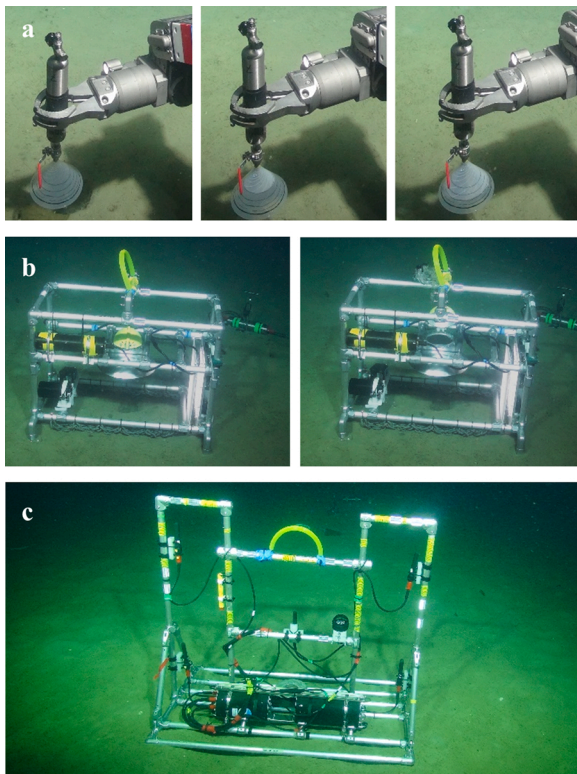


**Fig. 9.** Selection of methods employed to detect and/or characterise gaseous CO<sub>2</sub> in the water column. (a) Gas bubble sampling, with the ROV arm holding gas bubble sampler connected to an inverted funnel over a bubble stream. (b) Self-illuminated optical lander with bubble imaging and “rain gauge” bubble collector closed (left) and open (right) with gas escaping. (c) Hydrophone wall housing the passive acoustic setup.

originates from a leakage rather than a natural source (Dixon and Romanak, 2015). One way to do this is to ‘label’ the CO<sub>2</sub> in the storage reservoir with tracers. These are chemical constituents that are either inherent to the injected CO<sub>2</sub>, arising from natural processes within the reservoir, or have been purposely added to the injected CO<sub>2</sub>. In the STEMM-CCS release experiment inherent tracers ( $\delta^{13}\text{C}_{\text{CO}_2}$ ,  $\delta^{18}\text{O}_{\text{CO}_2}$ ) and added tracers (Kr, SF<sub>6</sub>, C<sub>3</sub>F<sub>8</sub>) were tested (Section 3.2). The added tracers had a significantly lower solubility in seawater than CO<sub>2</sub>, so the change in gas composition could be used to estimate the fraction of CO<sub>2</sub> that dissolved in the sediment pore waters and in the water column at different injection flow rates.

Gas was sampled using custom-built gas bubble samplers (GBS) (Corsyde, Germany) that were operated by the ROV manipulator arms. The GBS consisted of an inverted transparent funnel (0.7 l internal volume), inlet valve, stainless steel sample cylinder (0.5 l internal volume) and outlet valve (Fig. 9a). Markings on the funnel helped to identify the volume of gas collected over a given time period, providing an approximate flow rate from the bubble stream. Gas was usually collected once a day from (i) the gas rig sample point, (ii) ~10–15 cm above seabed bubble streams, and (iii) occasionally from ~0.9–2.7 m above seabed. The rig gas samples were used to identify any temporal variability of the CO<sub>2</sub>:tracer ratio in the injection gas so that changes in the gas composition of the bubble stream samples could be accurately computed. Gas samples from ~0.9–2.7 m above the seabed were collected to quantify the rates of CO<sub>2</sub> dissolution in the water column. In addition to the added tracer gases, methane (CH<sub>4</sub>), which was present in trace quantities in the released CO<sub>2</sub> gas, provided an independent tracer unaffected by potential variability of the tracer mixture injection system. An onboard flow-through Fourier-Transmission Infra-Red (FTIR) analyser (atmosFIR, Protea Ltd., UK) was used to measure CO<sub>2</sub>, CH<sub>4</sub>, SF<sub>6</sub>

and C<sub>3</sub>F<sub>8</sub> concentrations in the gas samples. Sub-samples for determination of the isotopic signatures ( $\delta^{13}\text{C}_{\text{CO}_2}$ ,  $\delta^{18}\text{O}_{\text{CO}_2}$ ) and Kr concentration were taken for analyses back onshore.

#### 4.2.3. Passive acoustics (hydrophone walls)

Measurements of the sounds of bubbles as they emerge from the seabed into the water column allows determination of the gas flux and the sizes of bubbles (Leighton and White, 2012).

In previous underwater bubble acoustic experiments, one hydrophone was used to take passive acoustic time series data, and the temporal data were used to quantify the gas flux (Bergès et al., 2015). In the STEMM-CCS experiment, this technique was extended by using an array of hydrophones. This allowed the location of the bubble streams to be identified. It also increased the range of the technique by enhancing the signal-to-noise ratio because a single-hydrophone-based passive acoustic technique is susceptible to underwater background noise, e.g., ship noise and sea surface noise (Leighton and White, 2012; Li et al., 2019). During the CO<sub>2</sub> release experiment the application of a hydrophone array and beamforming technique for potential CCS leakage monitoring was tested. The hydrophone array comprised five hydrophones fixed at different physical positions on a frame with a height of 1.10 m and a width of 1.36 m (Fig. 9c). The five hydrophones were linked to an acoustic recorder (RS-ORCA), which was used to archive the sound of bubbles emerging from the seabed. The passive system was programmed to make measurements at predetermined time intervals of 5 min on and 5 min off during the gas release experiment. These developments made it possible to improve the signal-to-noise ratio for flow rate quantification and single bubble detection, to localise the gas seep site, and to quantify the bubble size and gas flow rate for each seep.

#### 4.2.4. Active acoustics: Ship-based sonar and AUV-based sidescan sonar

Given the strong impedance contrast between water and gas, hydro-acoustics are very sensitive to the presence of gas bubbles in the water column. Hydro-acoustic sonar systems can be both ship- and AUV-based, depending on the required physical scale and resolution.

Hydro-acoustic data were collected during the JC180 cruise using the ship-mounted multi-beam Kongsberg EM710 and the single-beam Simrad EK60. The EM710 transmits a high frequency pulse in a fan shape beneath the vessel, surveying a large portion of the seafloor perpendicular to the ship’s track. The EK60 echo sounder transmits a single beam of 5 different monochromatic frequencies surveying a small portion of the seafloor and the water column directly beneath the ship. The multi-beam echosounder was used to survey a wide area around the experimental site to ensure all bubble streams were identified. The calibrated single-beam system was used to determine bubble stream properties, i.e., bubble size and mass flow rate, via modelling. Similar ship-based active acoustic measurements were made by RV *Poseidon* where a Simrad EK80 and EC150-3C transducer were mounted through the ship’s moon pool for echosound and current profile measurements. This system was used to observe bubble streams as well as to identify the location of the towed Video-CTD system.

To examine the surface features of the seafloor in greater detail, a Geoswath bathymetric sidescan sonar was mounted on the AUV. Surveys using the AUV were carried out prior, during and after the CO<sub>2</sub> release (Fig. 4). Similar to the multibeam system described above, an even wider, fan-shaped, outgoing sound pulse is transmitted by the sidescan sonar, and the backscatter returns are recorded as continuous signals on both sides of the instrument, in two sets of slightly offset receivers, enabling the calculation of water depth and seafloor reflectivity across the swath. The bubble streams could also be identified in the ‘water column’ section of the sidescan sonar records. The system operated at higher frequency than the ship systems, providing a finer resolution and more detail close to the seabed though with smaller footprint.



### 4.3. Detection of dissolved CO<sub>2</sub> in the water column

Dissolved CO<sub>2</sub> in the water column was measured in collected samples, in seawater pumped onto the ship (Section 4.3.1) and with in-situ instruments in the water column on mobile and fixed equipment. The flux of dissolved CO<sub>2</sub> from the seafloor was measured using incubation chambers deployed on the seafloor (Section 4.3.2). Dissolved CO<sub>2</sub> concentration and flux across the sediment-water interface in the vicinity of bubble streams was quantified with eddy covariance and the lab-on-chip gradient method (Sections 4.3.3 and 4.3.4). Measurements were also conducted with in-situ sensors mounted onto a towed frame (Section 4.3.1) and mounted directly onto the ROV and AUV (Sections 4.3.5 and 4.3.6).

#### 4.3.1. Discrete and continuous water sampling

Discrete water column samples were collected from both ships to detect the influence of the injected CO<sub>2</sub> gas on carbonate system parameters and/or on the dissolved tracer concentrations.

On board the RRS *James Cook*, the water column was sampled using Niskin bottles (6 × 1.7 L) mounted at the back of the ROV (Fig. 10a). Once a day, up to four Niskin bottles were fired between 1.5 and 2.5 m above seabed bubble streams and a further two bottles were fired close to the gas rig to establish a background value far from the bubble streams. These samples were used to determine concentrations of dissolved inorganic nutrients, TA, DIC, carbon and oxygen isotopes ( $\delta^{13}\text{C}_{\text{DIC}}$ ,  $\delta^{18}\text{O}_{\text{H}_2\text{O}}$ ), SF<sub>6</sub>, C<sub>3</sub>F<sub>8</sub> and Kr.

On board the RV *Poseidon*, a towed multipurpose Video-CTD water sampler rosette was used to sample the water column. This equipment was developed for detecting and monitoring gas-rich fluid seepage from the seafloor (McGinnis et al., 2011; Schmidt et al., 2015; Sommer et al., 2015) and for leakage rate estimation (Gros et al., 2019). The Video-CTD was equipped with Niskin bottles (10 × 10 L), a HD video camera, and additional sensors for pH (SBE27, Sea-Bird Electronics, Inc.) and dissolved CO<sub>2</sub> (HydroC-CO<sub>2</sub>, Kongsberg Maritime Contros). The towed Video-CTD water sampler rosette was used for (i) discrete water sampling using the Niskin bottles, (ii) continuous water sampling by pumped supply, and (iii) in-situ measurements of the partial pressure of CO<sub>2</sub> (pCO<sub>2</sub>). The Video-CTD was towed in bottom view mode (at ~1–5 m above seafloor) while the ship traveled at low speed (0.2–1 knots) following a random track pattern for ~10 h. The system was deployed during CO<sub>2</sub> release rates of 0, 6, 29, and 143 kg/day (Fig. 4). The natural background pCO<sub>2</sub> during deployments was determined by sampling in areas 700–2700 m from the release site. All data sets from in-situ sensor measurements were recorded online and were related to the ship's navigation data and weather data. Live HD video-streams and images were recorded for subsequent benthic characterisation. Discrete water samples were taken from the Niskin bottles for analyses of DIC, TA,  $\delta^{13}\text{C}_{\text{DIC}}$ , DOC, DON (dissolved organic nitrogen) and inorganic nutrients. In addition, seawater was continuously pumped from specific depths into an onboard Membrane Inlet Mass Spectrometer (MIMS) for real-time analysis of dissolved gases. Discrete samples for DIC, TA,

$\delta^{13}\text{C}_{\text{DIC}}$  and inorganic nutrient analyses were collected hourly from the pumped water supply and when the Video-CTD was above active bubble streams (confirmed by video image) to help calibrate the in-situ pH and pCO<sub>2</sub> sensor measurements.

#### 4.3.2. Benthic chambers

Benthic chambers are in-situ incubation chambers, which were used to quantify the flux of DIC across the sediment-water interface near the CO<sub>2</sub> bubble streams before and during the release experiment and to monitor the potential effect of the CO<sub>2</sub> release on the fluxes of other solutes. The chambers enclose and gently mix a known volume of benthic water and automatically collect water samples into glass syringes throughout the deployment for later analyses of a wide variety of solutes.

During the field experiment, two benthic chambers were deployed (Fig. 10b; McGinnis et al., 2014) for a total of 5 deployments (Fig. 4). The chambers were deployed by the ROV and inserted into the top few centimeters of the sediments to seal a fixed ~6 l volume of water above the sediment. By monitoring the evolution of solute concentrations within this incubated volume over 27–38 h, their fluxes across the sediment-water interface were quantified. The benthic chambers included an O<sub>2</sub> optode (Aanderaa, Xylem, USA) and temperature sensors for continuous collection of in-situ data. During each deployment, eight water samples of ~46 ml were automatically collected into glass syringes by the chamber system. These samples were later analysed in the laboratory for dissolved gases, nutrients, stable isotopes ( $\delta^{13}\text{C}_{\text{DIC}}$ ,  $\delta^{18}\text{O}_{\text{H}_2\text{O}}$ ), and TA.

#### 4.3.3. Eddy covariance

The rapid dissolution of CO<sub>2</sub> bubbles as they emerge from the seabed generates a strong vertical gradient of hydrogen ions (which cause low pH) and DIC (Zeebe and Wolf-Gladrow, 2001). The interaction of currents with this source induces turbulent mixing. The vertical component of this mixing drives a net upwards flux of hydrogen ions and DIC from the seafloor. The eddy covariance technique quantifies the upward flux by simultaneously measuring the pH and 3D velocity of a small volume of water at high frequency (e.g., 5 Hz). The implementation for the STEMM-CCS project followed published work which used this technique for benthic biological O<sub>2</sub> (Berg et al., 2003) and CO<sub>2</sub> (Long et al., 2015) production. Because pH eddy covariance is sensitive enough to quantify the naturally-occurring benthic biotic CO<sub>2</sub> flux, it was expected to be exceedingly sensitive to a CO<sub>2</sub> bubble stream. During the release experiment, both O<sub>2</sub> and pH eddy covariance fluxes were determined. Turbulent fluctuations in velocity were measured with an acoustic Doppler velocimeter (Nortek, Norway), pH with a fast-response pH ion sensitive field effect transistor (ISFET, Microsensors Switzerland), and O<sub>2</sub> with an optode minisensor (PyroScience, Germany). The instruments were mounted to the fiberglass EC/gradients lander frame (Fig. 10d). The technical development for the application of eddy covariance to the quantification of the CO<sub>2</sub> release included a flow-through housing with an integrated, minimally stirring-sensitive reference developed for the

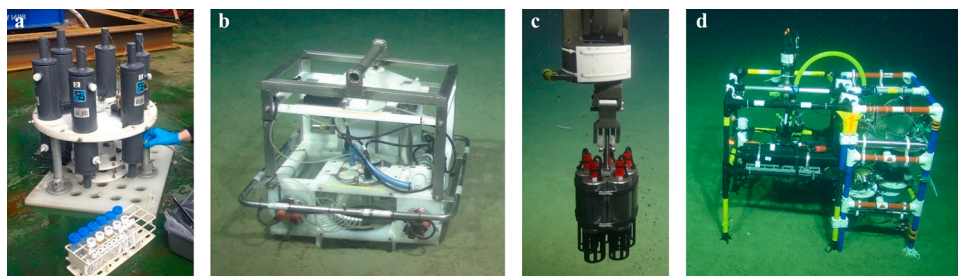


**Fig. 10.** Selection of methods employed for measuring dissolved CO<sub>2</sub> in the water column. (a) Niskin bottles for water sampling from the ROV. (b) Benthic chamber for measuring benthic fluxes. (c) pH optode sensors held in the bubble stream by the ROV's manipulator arm. (d) EC/gradients lander for eddy covariance and lab-on-chip chemical gradient measurements.



ISFET sensor. Flow was driven by an electronically-controlled gear pump that periodically reversed to flush debris that would otherwise clog the flow. Measurements were made 16 cm above the seafloor, 2.6 m south of the centre of the release site (Fig. 4). Complementary carbonate system parameters were obtained from lab-on-chip sensors on the same instrument frame (Section 4.3.4). The payload limitation of the ROV limited the maximum battery capacity of the landers, so two identical instrument frames were developed and swapped every 48 h before the batteries ran down. This allowed us to acquire a near-continuous time-series of observations during the CO<sub>2</sub> release.

The eddy covariance technique measured vertical flux at a single point located downstream of the source. Therefore, the measured flux represents only a small portion of the total release. To estimate the total release of DIC, the measured velocity, flow direction, and pH were combined with a modelled distribution of CO<sub>2</sub> dissolution above the seafloor.

#### 4.3.4. In-situ chemical gradient measurements

As CO<sub>2</sub> bubbles dissolve in the water column, they cause a strong drop in pH and an increase in DIC near the seafloor. Miniaturised spectrophotometric sensors measuring pH (R  rolle et al., 2013) and TA, and a conductometric sensor for measuring DIC directly, monitored these carbonate parameters. Spectrophotometric sensors for measuring nitrate (Beaton et al., 2012) and phosphate (Clinton-Bailey et al., 2017) were included to characterise any background changes in DIC due to biological activity.

These sensors were all "lab-on-chip" (LOC) devices: autonomous miniaturised instruments which perform chemical assays in-situ with low power and reagent consumption. The sensors draw in seawater, mix it with chemical reagents, and measure the reaction products either optically or electrochemically. The TA and DIC sensors were custom-developed for this CO<sub>2</sub> release experiment.

One LOC sensor for each of the above parameters was mounted on each EC/gradients lander (Fig. 10d). Each sensor sampled from two inlets: a lower inlet located 18 cm above the seafloor and a higher inlet located 87 cm above the seafloor. Each sensor continuously alternated between the two sample inlets to characterise the vertical concentration gradient in each parameter at sample intervals of 5–15 min depending on the sensor. The EC/gradients landers were deployed throughout the release experiment, yielding a nearly-continuous dataset from before the gas was turned on until the day it was turned off (Fig. 4). The data from these LOC sensors, along with measurements of the current, can be used to quantify the dissolved fraction of the CO<sub>2</sub> release by estimating the total excess DIC content of the water as it passes over the lander.

#### 4.3.5. Chemical mapping with the ROV

The ROV was used as a vehicle for deployment and positioning of equipment at the seafloor as well as a survey instrument. To determine the spatial extent of the plume, several overnight dives were used to perform three-dimensional chemical surveys of the experiment site with LOC sensors and optodes. ("Plume" here refers to water from the vicinity of the bubble streams that is characterised by elevated DIC concentration and reduced pH as a result of the CO<sub>2</sub> gas dissolving in the seawater.) While ROVs cannot be used as a long-term monitoring approach without a ship present, these measurements enabled the creation of maps of the plume which could be used to validate models of the release.

A suite of five spectrophotometric LOC sensors were used to measure carbonate system parameters and nutrients (see Section 4.3.4). These were mounted to a removable rack on the back of the ROV, visible in the bottom-left corner of the vehicle in Fig. 3a. A pump at the front of the ROV supplied seawater to the LOC sensors for analysis. A live data stream was delivered via the ROV tether to provide real-time results from the LOC sensors to the ship allowing the operators to adjust survey plans in real-time during the surveys if required.

The pH optodes were similar to those utilised for sediment pore

water analysis (Section 4.1.3). Unlike the sediment optodes, however, these pH optodes utilised sensor spots on a screw-on cap adaptor attached to the logger in a titanium pressure housing (63 mm diameter, 270 mm length) designed by PyroScience GmbH (Germany). The optodes were held by the ROV's robotic arm during the surveys (Fig. 10c). Oxygen optodes were also deployed in the same set up for reference purposes.

Chemical surveys were performed with LOC sensors and pH optodes operating simultaneously. Longitudinal (north-south) surveys were performed with the ROV moving from directly above the bubbles to 10 m downstream at altitudes of 1.5 and 3.5 m. A lateral (east-west) survey was performed at 6 m downstream from the bubbles and 1.2 m altitude to map the distribution of the plume perpendicular to the current. The LOC sensors also gathered data on all ROV dives while the ROV was completing other tasks in and around the experimental site.

#### 4.3.6. pH sensors on AUV

To collect spatial data on the pH distribution over the larger experimental region a high temporal resolution pH sensor (Deep SeaFET<sup>TM</sup>, Sea-Bird Scientific, USA) was mounted on to the AUV (Teledyne, USA) (Fig. 3b). This pH sensor uses an ion sensitive field effect transistor (ISFET) to measure pH changes. This sensor was selected because of its high sample frequency of 1 Hz and its depth rating of 2000 m. The sensor was mounted externally on the Gavia AUV using a custom-made bracket, fabricated from syntactic foam, designed to minimise drag.

The SeaFET recorded data on seven dives over the course of the experiment using a variety of dive track patterns. To avoid any interactions with the CO<sub>2</sub> release equipment at the seafloor, the AUV had to remain at a relatively high altitude (4–7.5 m) when it was close to the CO<sub>2</sub> release site.

## 5. Outcomes and discussion

This section summarises the general outcomes of the release experiment activity and the lessons learnt. An overview of the position and timing of the ships, vehicles, deployed equipment, and CO<sub>2</sub> injection flow rates throughout the experiment is given in Fig. 4. For detailed results, the reader is referred to the specialised papers, which can largely be found in this special issue.

### 5.1. Baseline measurements and site characteristics

In environmental monitoring a robust understanding of the systems' natural variability is essential to differentiate between a potential leak signal and an anomaly caused by natural phenomena or unrelated human activity.

Results from the environmental baseline studies showed that the experimental site, and wider Goldeneye area, was located on a relatively flat seabed with a gentle slope, dipping east-north-east towards a broad depression termed the Witch Ground Basin (Strong et al., 2020). The near-surface sediments at Goldeneye had a sand content of ~70 %, decreasing to ~30 % by 120 cm depth below seabed, and a porosity between 0.4 and 0.6 (Dale et al., 2020). The organic carbon content was low (0.6 %). Benthic respiration rates at Goldeneye were typical for coastal margins (~6 mmol/m<sup>2</sup>/d of O<sub>2</sub>). Stoichiometric relationships between the fluxes of sulfate, ammonium and alkalinity in the pore waters have the potential to serve as diagnostic indicators for CO<sub>2</sub> leakage at Goldeneye (Dale et al., 2020).

The benthic fauna studies revealed that the experimental site was a fairly typical habitat for the continental shelf surrounding the British Isles (Strong et al., 2020). The benthic macrofauna study identified 10, 207 individuals from 264 taxa in 13 phyla in 76 box cores. Based on abundance, 70 % of individuals were annelids, 11 % molluscs, 8 % arthropods, 7.5 % echinoderms and 2.3 % nemertean. The most significant factor influencing benthic community structure was sediment type, in particular whether the substratum was muddy sand or sandy mud.

Lesser impacts on the benthic macrofauna from trawling and the presence of pockmarks were also evident. The baseline imaging survey revealed that heterogeneity in the megafaunal community at the Goldeneye area was low. A total of 24 morphotypes were observed at these sites (Hosking et al., 2020; Schmidt et al., 2020; STEMM-CCS D2.7, 2020). The crustacean, *Nephrops norvegicus*, the subject of some mapping work (see Section 2.2.3), was one of the most common megafaunal organisms observed. The diversity and composition of the megafaunal community was not significantly different between the experimental site and the background site distant from it. These data suggest that a robust baseline assessment design should consider spatial variability for different organism size classes (e.g., macrofauna and megafauna).

Hydrographical data gathered before and during the release experiment by the NOC baseline lander (Fig. 13a) show that the experimental region is dominated by tides (tidal range 1.7 m) and by associated currents with a very narrow tidal ellipse with the major axis aligned in the north-south direction. The maximum current ranged from approximately 10–25 cm/s at 16 cm and 15–30 cm/s at 120 cm above the seafloor (Fig. 13b). The currents remained within 30 degrees of north to south 80 % of the time, allowing for occasional quasi-steady-state conditions for measurements. Consequently, landers and stationary instruments were located on the seabed upstream and downstream of bubble streams for half of their deployment time. The instruments thus effectively measured “background” data during the upstream period, and CO<sub>2</sub> release during the downstream period. The varying direction of current meant that physically stationary landers could examine the spatial aspects of the plume from a temporal signal, as the currents caused the plume of dissolved CO<sub>2</sub> to sweep across the instruments. This is evident in the chemical time series data from the experiment, described in other papers within this special issue (Koopmans et al., 2020; Schaap et al., 2020). This underscores the importance of knowledge of the local hydrography when determining optimal lander positioning for environmental monitoring.

Water column carbonate system baseline data acquired during three expeditions along with historical data from the Goldeneye area show that near the seafloor the carbonate system varies as a function of seasonality, tidal cycles, and weather events such as storms. On the seasonal scale, drops in pH and build-up of pCO<sub>2</sub> in the near-bottom waters are dominated by cumulative remineralisation of sinking organic matter over the course of the year while the breakup of water column stratification reduced bottom water pCO<sub>2</sub> and increased pH. The annual range in pH was ~0.15 units and the annual range in pCO<sub>2</sub> was about 160 µatm. High-resolution pH and pCO<sub>2</sub> measurements obtained from the seabed landers suggest that tides drive short-term pH and pCO<sub>2</sub> variability in bottom waters of, respectively, ±0.008 and ±1.5 µatm. Storm events led to abrupt and pronounced changes in carbonate chemistry parameters of up to 0.02 pH units and 30 µatm in pCO<sub>2</sub> over a relatively short time (6 h) interval. Crucially, the results suggest that the natural short-term variations in pH are smaller than the proposed theoretical ΔpH criteria to effectively detect anomalies (Blackford et al., 2017). The application of multilinear regression analysis and co-variance relationships between water column parameters allowed the establishment of robust pCO<sub>2</sub>:O<sub>2</sub> seasonal thresholds capable of assisting with the identification of anomalies that would be indicative of non-natural sources of CO<sub>2</sub> (Esposito et al., 2020). The comparison of STEMM-CCS data with historical data from the Goldeneye area show that the carbonate system baseline in seawater has shifted due to invasion of increasing levels of anthropogenic atmospheric carbon dioxide. This would also need to be taken into account with, for example, stoichiometric analysis (Esposito et al., 2020; Martínez-Cabanas et al., 2020; Omar et al., 2020).

## 5.2. Outcomes of release experiment

The location of the experimental site was guided by the baseline site mapping of the oil and gas infra-structure in the Goldeneye area such as wellheads and pipelines (Strong et al., 2020, Fig. 2). Ultimately, the CO<sub>2</sub>

container and the experimental site were located approximately 900 m south of the Goldeneye platform, i.e., beyond the range of influence of oil and gas infrastructure.

The properties of the sediment were conducive for inserting the pipe and releasing the gas. The pipe insertion occurred without technical complications, taking only 24 min, and the insertion rig was back on deck within ~1 h. After maintenance of the gas release system to address gas release performance issues, the CO<sub>2</sub> rig was successfully re-deployed, the gas supply was tested, and the flexible hose was connected to the pipe inlet within a day and without major issues.

The CO<sub>2</sub> was turned on at 15:19 on 11 May 2019 and the flow rate was set to 6 kg/d. Bubbles were observed emerging from the sediments within the 30 min it took the ROV to arrive at the release site. The gas injection flow rate was turned up incrementally over the course of the experiment to 14, 29, 86, and finally 143 kg/d (Fig. 11). The CO<sub>2</sub> release system was built to allow maximum injection flow rates of 286 kg/d (100 normal L/min) but following issues with the performance of the gas regulator it was decided to keep the maximum injection flow rate at 143 kg/d. The technical challenge of injecting very low amounts of tracer gas into the CO<sub>2</sub> gas flow meant that the CO<sub>2</sub>:tracer ratio fluctuated significantly at low injection rates, but stabilised at higher injection rates (≥29 kg/d).

Three separate streams of bubbles were visible at the lowest flow rate. Over the course of the experiment several further bubble streams were identified as the gas flow was increased, with some bubble streams occurring intermittently (see examples of bubble streams visible in Fig. 12a). All of the observed bubble streams occurred within a 4 m radius of the expected position of the pipe outlet, though most were clustered ~2 m to the south of this point (Fig. 4) (Strong et al., 2020). Dissolution of the bubbles in the water column was observed with the video footage from the ROV; no bubbles were visible to the camera at heights of >8 m above the seabed.

Most sediment cores were collected away from the pre-existing points of gas release and coring did not appear to modify the flux of CO<sub>2</sub> gas across the seabed. Some cores were collected from a point where there was already gas contained within the sediments (i.e., immediately below or next to pre-existing bubble streams). In these cases, the collection of the cores was associated with a slight change in where the CO<sub>2</sub> was emitted from the seafloor but no significant change in flow rate.

The main findings of each of the different techniques for CO<sub>2</sub> detection, attribution, and quantification are as follows:

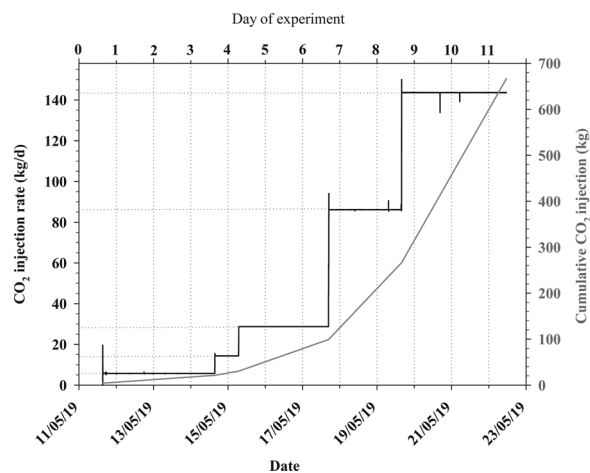
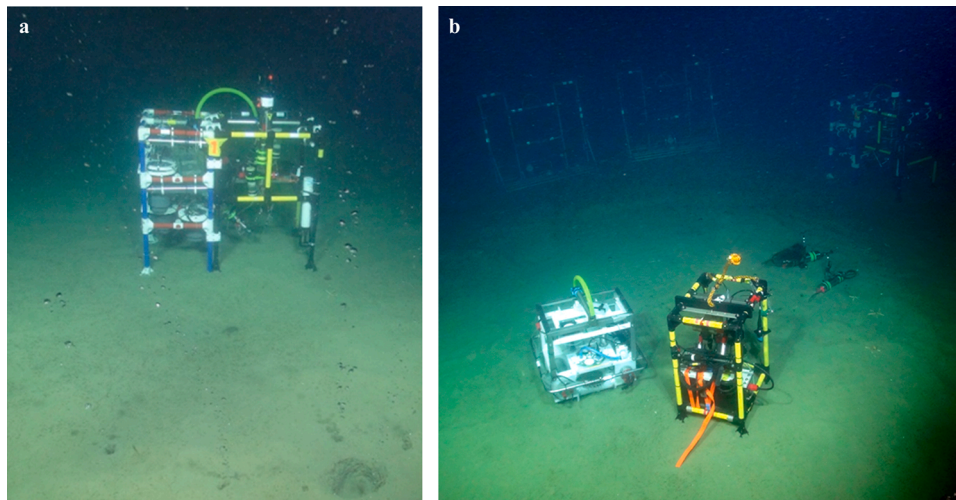
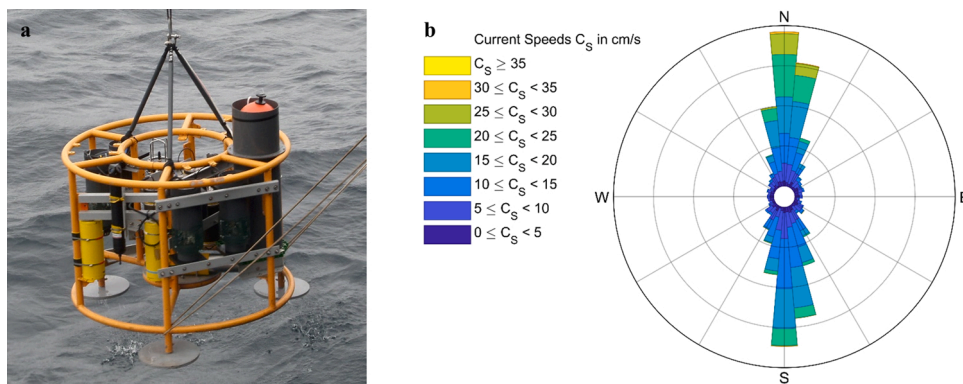


Fig. 11. Gas injection during the release experiment. Injected gas mass flow rates (black solid line, left y-axis) and cumulative gas mass (grey solid line, right y-axis) injected over time (day of experiment (top x-axis) and respective date (bottom x-axis)).



**Fig. 12.** Experimental site. (a) Example of multiple bubble streams originating from small pockmarks visible in the sediment observed on day 8 of the experiment at a  $\text{CO}_2$  injection rate of 86 kg/d. (b) Example of equipment positioning at the experimental site. Benthic chamber and sediment microprofiler in the foreground, the sediment optodes along the middle and right, and hydrophone walls and benthic boundary layer lander in the background.



**Fig. 13.** Measurements of currents during the release experiment. (a) NOC baseline lander used for current measurements at 1.2 m altitude above the seabed. (b) Current data. The radial length of each segment indicates the relative frequency of the current direction with the current speed in cm/s is indicated by the colour.

- Sediment geochemistry: In the sediments close to the bubble streams, the impact of injected  $\text{CO}_2$  was detectable based on changes in the pore water chemistry, mainly associated with carbonate dissolution (Lichtsschlag et al., 2020a).
- Sediment microprofiler: The microprofiles in the bubble streams were highly variable, with porewater pH values as low as 5. An increase in temperature could be attributed to exergonic reactions between  $\text{CO}_2$  and sediment pore waters and  $\text{CO}_2$ -sediment weathering (reactions with calcite and silicate). The pore water chemistry and temperature effects were only detectable within a few cm from the bubble streams (de Beer et al., 2021).
- Sediment optodes: The sediment optodes showed a clear increase in temperature and a decrease in pH at a distance of 1 m and 1.4 m from the leakage. At a distance of 4 m and 7 m the values stayed constant. The deviation in temperature was easier to detect because the background values did not drift.
- Gas bubble imaging: Cameras on the seabed lander identified bubbles from a single seep with  $\sim 80\%$  of the bubbles ranging in size from 0.2 to 0.5 cm in radius, with most around 0.3 cm. The optically derived bubble size distribution was successfully used to quantify the gas flow rate of an individual bubble stream into the water column (Li et al., 2020).
- Gas bubble sampling: Detection of the added tracer gases in gas samples taken from bubble streams confirmed the source of the gas to be the injected  $\text{CO}_2$ . Tracer gas analyses were successfully used to quantify the amount of  $\text{CO}_2$  that remained in the sediment due to  $\text{CO}_2$  dissolution in pore waters. The total leakage rates were successfully determined using gas bubble samplers (Flohr et al., 2020).
- Passive acoustics: The frequency of the bubbles recorded by passive acoustic methods allowed the determination of bubble radii, with a range of 0.15 to 0.30 cm, consistent with gas bubble imaging. Inversion of the hydrophone data facilitated an estimate of the total gas flux into the water column (Li et al., 2019, 2020).
- Active acoustics: The chirp sub-bottom profiler on the Gavia AUV resolved the evolution of gas migration pathways throughout the experiment via enhanced reflectors, shadowing, variations in attenuation and root mean square amplitude and unit thickness. Particularly noteworthy was the imaging of the development of a gas pocket as injection rate increased, and its later decline, with the development of open fluid flow conduits (Roche et al., 2020).
- Water sampling: Analyses of carbonate chemistry parameters throughout the water column detected drops in pH values and sharp increases in  $\text{pCO}_2$  within 8 m of the bubble streams at low tide. The influence of the injected  $\text{CO}_2$  was confirmed by anomalies in the stoichiometric ratio of  $\text{O}_2$  to  $\text{pCO}_2$  relative to baseline values (Esposito et al., 2020; Martínez-Cabanas et al., 2020).
- Video-CTD: Video imaging and  $\text{pCO}_2$  sensor data acquired with the Video-CTD detected visible bubble streams and peaks in sensor signal resulting from the experimentally released  $\text{CO}_2$ . Deviations from the time-varying baseline were related to the injected  $\text{CO}_2$  flow



rate, and combined with modelling, which could potentially be used to quantify leakage rate (Gros et al., 2020).

- **Benthic chambers:** Benthic chambers deployed 0.5–1.0 m away from bubble streams did not detect any flux of experimentally-derived CO<sub>2</sub> in the form of excess DIC across the sediment-water interface, within the limit of detection of the analytical methods. This is tentatively interpreted as a sign that during the early period of CO<sub>2</sub> release, most of the CO<sub>2</sub> escaping into the water column was in gas form (Gros et al., 2020).
- **Eddy covariance:** The eddy covariance system detected a clear signal of hydrogen ion production due to CO<sub>2</sub> gas dissolution at the lowest CO<sub>2</sub> injection rate and throughout the experiment. It also quantified naturally-occurring biotic CO<sub>2</sub> production in surrounding sediments. Therefore, pH eddy covariance is a highly sensitive technique for the detection of a seafloor source of CO<sub>2</sub> (Koopmans et al., 2020).
- **In-situ chemical gradient measurements:** This technique showed a strong drop in pH whenever the current direction caused the CO<sub>2</sub>-enriched water from the plume to contact the sensors. When coupled with simple models, this technique could quantify the emission of CO<sub>2</sub> into the water column at all but the lowest release rate (Schaap et al., 2020).
- **Chemical mapping with the ROV:** Each of the three types of pH sensors mounted on the ROV detected the plume. Plume mapping confirmed the highly-localised nature of the plume and the impact of currents on the shape and orientation of the plume. This highlights the importance of considering currents when designing a survey path for vehicles searching for plumes (Monk et al., 2020).
- **pH sensors on the AUV:** The AUV collected pH data over a much wider spatial area than the ROV but had to maintain an altitude of >4 m above the seabed to avoid the gas rig infrastructure. The pH sensors were not able to detect the plume at this height. This result is consistent with models, which predicted the plume would not be detectable at distances of >2 m above the seabed. However, when the SeaFET pH sensor was removed from the AUV and mounted on the ROV it detected the plume, demonstrating that the method should work in an environment where the AUV can maintain a lower altitude.

In summary, during the experiment, the released CO<sub>2</sub> was detectable in its gaseous and dissolved form in both the sediments and the water column. In the sediments close to the bubble streams, the impact of injected CO<sub>2</sub> was detectable based on changes in the pore water chemistry, as a temperature increase in the pore water and in gas form from chirp measurements. Gas bubbles in the water column were detectable optically and acoustically, and CO<sub>2</sub> that dissolved in the water column created a distinctive signal that was detectable chemically by in-situ and lab-based methods.

### 5.3. Relevance of experimental outcomes for environmental monitoring of offshore subseafloor CO<sub>2</sub> storage

While no acceptable leakage rates have been legislated yet for offshore CO<sub>2</sub> storage, a range of acceptable leakage rates could be estimated using the rate of 0.01 % reservoir loss per year proposed in the literature (e.g., Hepple and Benson, 2005). If applied to the proposed injection rate (~1 Mt/yr) and duration (20 years) at Goldeneye (Dean and Tucker, 2017), this would yield a range of acceptable leakage rates of 274 kg/d after the first year of injection and 5480 kg/d after 20 years of injection when full storage capacity is reached. During the STEMM-CCS release experiment CO<sub>2</sub> gas was injected at flow rates from 6 to 143 kg/d. Around 50 % of the injected CO<sub>2</sub> escaped across the seabed into the water column, which was well below these estimated acceptable leakage rates. The injected CO<sub>2</sub> was detected in all its forms, i.e., gaseous and dissolved in the sediments, and gaseous and dissolved in the water column. As CO<sub>2</sub> leakage is unlikely to be continuous over the whole reservoir area but is rather expected to be preferentially

transported through small focused fractures and faults or through poorly-sealed, abandoned wells (IPCC, 2005), both the flow rates and the type (point-release) of our simulated leakage are relevant for real-world scenarios.

A major factor in the design of the experiment was the use of a range of approaches, which mitigated risk and offered a balance between the quantity and quality of the gathered data. The combination of mobile and fixed-position methods provided both high-accuracy data and spatial coverage. Measuring the CO<sub>2</sub> within the sub-seafloor and in its gaseous and dissolved form in the water column allowed quantification of the CO<sub>2</sub> fraction remaining in the sediment versus the CO<sub>2</sub> fraction that escaped into the water column. This knowledge is important for designing future monitoring programmes as well as for informing and improving models.

The radically different approaches, relying on complementary signals from optical, acoustic, and chemical changes, meant that biases or limitations in any one technique could be identified and accounted for. Crucially, in a real-world scenario, the use of complementary approaches will help to minimise the chances of detecting false positives. The combination of novel techniques, adapted versions of existing techniques, and well-proven standard techniques allowed for high-frequency and high-spatial-coverage data to be cross-checked and quality-controlled and also made the release experiment a suitable demonstration opportunity for new technologies developed specifically for STEMM-CCS. The use of in-situ technology meant informed decisions could be made in a responsive manner. We anticipate that any future environmental monitoring programme may wish to consider a similarly balanced set of approaches. However, the monitoring technologies developed in STEMM-CCS are just one element (the environmental) of a comprehensive risk-based Measurement, Monitoring and Verification (MMV) programme an operator has to develop, which includes the subsurface and wells (Dean and Tucker, 2017). Consequently, any deployment of the STEMM-CCS technologies will also depend largely on the risk features identified in the subsurface. Many techniques utilised in this experiment are complex and not all the technology is, as yet, commercially available or familiar to the wider research community. To support its dissemination, an online tool for supporting decisions about monitoring techniques has been prepared by the project consortium (; Lichtschlag et al., 2020b) and is available online at [www.stemm-ccs.eu/monitoring-tool](http://www.stemm-ccs.eu/monitoring-tool). This tool indicates the level of operational expertise and cost of individual techniques, as well as their spatial and temporal resolution and overall utility.

The plume modelling conducted prior to the field experiment indicated that any CO<sub>2</sub> that escaped across the seabed and into the overlying water column would be dispersed and diluted very rapidly by natural mixing driven by turbulence and tidal motion. As a result, it was expected that the resulting chemical changes would be below the threshold which would present any environmental risk (Blackford et al., 2020). Whilst this result facilitated the consenting process for the experiment, it also highlighted that the deployment of sensors had to be spatially meticulous in order to maximise the utility of the experimental outcomes (see photo of seafloor equipment layout, Fig. 12b).

Given the likely small spatial extent of a plume and its rapid dilution away from its seabed source, future monitoring strategies will need to be supported by model simulations, e.g., coupled hydrodynamic-biogeochemical models (e.g., Blackford et al., 2017; Lessin et al., 2016, 2018; Vielstädte et al., 2019) which can provide optimal deployment strategies of sensors or efficient vehicle trajectories for detection, location, and quantification of leakages (Alendal et al., 2017; Alendal, 2017; Hvidevold et al., 2015; Gundersen et al., 2018; Oleynik et al., 2018).

## 6. Conclusions

The STEMM-CCS project completed a large-scale field experiment in the central North Sea designed to simulate and detect an unintended

emission of CO<sub>2</sub> from a CO<sub>2</sub> storage site. A unique experimental design enabled the release of CO<sub>2</sub> into the shallow sediments and a range of novel and standard methods were applied to detect and quantify the release of CO<sub>2</sub>. The aim of this paper was to synthesise the work done prior to and during the CO<sub>2</sub> release experiment. Overall, the experiment was a major success. The CO<sub>2</sub> release system was able to deliver flow rates over more than an order of magnitude (6–143 kg/d) to test relevant leakage rate scenarios. The outcomes of the experiment demonstrate that a sub-seafloor release of CO<sub>2</sub>, mimicking a leakage from an offshore CO<sub>2</sub> storage site, can be reliably achieved and can serve as a test bed for trialing new technologies and techniques. It further demonstrates that such a release can be detected, attributed, and quantified using multiple different approaches.

### Author contributions

Conceptualisation and management of overall project was done by EA, GA, CBe, JBl, SB, JBu, BC, AD, DdB, MDea, MHa, MHo, VH, RJ, TL, AL, PL, SL, JM, MM, HR, CS, KS, MS, SS, PW, SW, and DC.

Design and implementation of experimental work was done by AF, AS, EA, MA, JBl, CBö, SB, RB, JBu, LC, BC, AD, DdB, CD, MDew, SE, ME, MF, JF, AG, JG, MHa, RH, MHo, BH, VH, DK, EK, TL, JL, AL, PL, SL, MMC, JM, TM, SM, AO, SP, DP, CP, KP, BR, US, KS, MS, SS, JS, JT, BU, JWa, PW, RW, HW, JWY, and DC.

AF and AS co-led the writing of the paper; contributions to writing and revising were also provided by EA, GA, JBl, CBö, SB, JBu, BC, AD, DdB, MDew, JD, ME, JG, RH, MHo, VH, RJ, DK, EK, TL, JL, AL, SL, SM, SP, CP, BR, KS, JS, PW, and DC.

### Funding

The STEMM-CCS project has received funding from the European Union's Horizon 2020 research and innovation programme under grant agreement No. 654462.

Other work which contributed to this experiment has been funded by the UK's Natural Environmental Research Council: the SPITFIRE project, grant number NE/L002531/1; the Climate Linked Atlantic Sector Science project, funded through the single center national capability programme grant number NE/R015953/1; the Carbonate Chemistry Autonomous Sensor System (CarCASS) project, grant number NE/P02081X/1. Further funding was received from Bayesian Monitoring Design (BayMoDe), funded by the Research Council of Norway through the CLIMIT programme, project 254711; Act on Offshore Monitoring (ACTOM), funded through the ACT programme (Accelerating CCS Technologies Project) Horizon2020 project No 294766; and the Max Planck Society for Advancement of Science, Germany.

### Declaration of Competing Interest

The authors declare that they have no known competing financial interests or personal relationships that could have appeared to influence the work reported in this paper.

### Acknowledgements

We would like to acknowledge the hard work, enthusiasm, and professionalism of the captains, crews, and operators of the RRS *James Cook*, the RV *Maria S. Merian*, the RV *Poseidon*, the ROV *Isis* and the AUV *Gavia*, who made the experiment possible. In addition, the authors would like to thank the following who enabled the project and experiment to take place:

From the University of Southampton: Kate Davis and John Davis; from the Ocean Technology & Engineering Group, National Oceanography Centre: Alexander Beaton, Chris Cardwell, Anthony Kenny, Urska Martincic, Steven Shorter, and Daisy Tong; from GEOMAR Helmholtz Centre for Ocean Research Kiel: Anke Bleyer, Andrea Bodenbinder,

Sergiy Cherednichenko, Bettina Domeyer, Florian Ever, Isabelle Meckelburg, Gaby Schüßler, Regina Surberg, Matthias Türk, Asmus Petersen, Christine Utecht; from the Max Planck Institute for Marine Microbiology: Volker Meyer and Paul Färber; from Cellula Robotics Ltd.: Mark Wells; and the staff at Air Liquide UK Ltd., Bronkhorst UK Ltd., Cellula Robotics Ltd., City Gas EOOD, Corsyde International GmbH, DG Pipe Services Ltd., J & J Engineering (Southampton) Ltd., Protea Ltd., and Sourceways Ltd. We also thank two anonymous reviewers for their constructive comments.

### Appendix A. Supplementary data

Supplementary material related to this article can be found, in the online version, at doi:<https://doi.org/10.1016/j.ijggc.2020.103237>.

### References

- Achterberg, E.P., Esposito, M., 2018. RV POSEIDON Fahrtbericht / Cruise Report POS527 - Baseline Study for the Environmental Monitoring of Subseafloor CO<sub>2</sub> Storage Operations, Kiel - Kiel (Germany), 15.8 - 3.9.2018. GEOMAR Helmholtz-Zentrum für Ozeanforschung, Kiel, Germany.
- Alendal, G., 2017. Cost efficient environmental survey paths for detecting continuous tracer discharges. *J. Geophys. Res. Oceans* 122, 5458–5467.
- Alendal, G., Drange, H., 2001. Two-phase, near-field modeling of purposefully released CO<sub>2</sub> in the ocean. *J. Geophys. Res. Oceans* 106, 1085–1096.
- Alendal, G., Blackford, J., Chen, B., Avlesen, H., Omar, A., 2017. Using bayes theorem to quantify and reduce uncertainties when monitoring varying marine environments for indications of a leak. *Energy Procedia* 114, 3607–3612.
- Artoli, Y., Blackford, J.C., Butenschön, M., Holt, J.T., Wakelin, S.L., Thomas, H., Borges, A.V., Allen, J.I., 2012. The carbonate system in the North Sea: sensitivity and model validation. *J. Mar. Syst.* 102–104, 1–13.
- Aßmann, S., Frank, C., Körtzinger, A., 2011. Spectrophotometric high-precision seawater pH determination for use in underway measuring systems. *Ocean. Sci.* 7, 597–607.
- Beaton, A.D., Cardwell, C.L., Thomas, R.S., Sieben, V.J., Legiret, F.-E., Waugh, E.M., Statham, P.J., Mowlem, M.C., Morgan, H., 2012. Lab-on-chip measurement of nitrate and nitrite for in situ analysis of natural waters. *Environ. Sci. Technol.* 46, 9548–9556.
- Berg, P., Røy, H., Janssen, F., Meyer, V., Jørgensen, B.B., Huettel, M., de Beer, D., 2003. Oxygen uptake by aquatic sediments measured with a novel non-invasive eddy-correlation technique. *Mar. Ecol. Prog. Ser.* 261, 75–83.
- Berges, B.J.P., Leighton, T.G., White, P.R., 2015. Passive acoustic quantification of gas fluxes during controlled gas release experiments. *Int. J. Greenh. Gas Control.* 38, 64–79.
- Berndt, C., Elger, J., Böttner, C., Gehrman, R., Karstens, J., Muff, S., Pitcairn, B., Schramm, B., Lichtschlag, A., Völsch, A., 2017. RV MARIA S. MERIAN Fahrtbericht / Cruise Report MSM63 - PERMO, Southampton - Southampton (U.K.) 29.04.-25.05.2017. GEOMAR Helmholtz-Zentrum für Ozeanforschung Kiel, Kiel.
- Blackford, J., Stahl, H., Bull, J.M., Berges, B.J.P., Cevatoglu, M., Lichtschlag, A., Connelly, D., James, R.H., Kita, J., Long, D., Naylor, M., Shitashima, K., Smith, D., Taylor, P., Wright, I.C., Akhurst, M., Chen, B., Gernon, T.M., Hauton, C., Hayashi, M., Kaieda, H., Leighton, T.G., Sato, T., Sayer, M.D.J., Suzumura, M., Tait, K., Vardy, M.E., White, P.R., Widdicombe, S., 2014. Detection and impacts of leakage from sub-seafloor deep geological carbon dioxide storage. *Nat. Clim. Chang.* 4, 1011–1016.
- Blackford, J., Bull, J.M., Cevatoglu, M., Connelly, D., Hauton, C., James, R.H., Lichtschlag, A., Stahl, H., Widdicombe, S., Wright, I.C., 2015. Marine baseline and monitoring strategies for carbon dioxide capture and storage (CCS). *Int. J. Greenh. Gas Control.* 38, 221–229.
- Blackford, J., Artioli, Y., Clark, J., de Mora, L., 2017. Monitoring of offshore geological carbon storage integrity: implications of natural variability in the marine system and the assessment of anomaly detection criteria. *Int. J. Greenh. Gas Control.* 64, 99–112.
- Blackford, J., Alendal, G., Avlesen, H., Brereton, A., Cazenave, P.W., Chen, B., Dewar, M., Holt, J., Phelps, J., 2020. Impact and detectability of hypothetical CCS offshore seep scenarios as an aid to storage assurance and risk assessment. *Int. J. Greenh. Gas Control.* 95, 102949.
- Botnen, H.A., Omar, A.M., Thorseth, I., Johannessen, T., Alendal, G., 2015. The effect of submarine CO<sub>2</sub> vents on seawater: implications for detection of subsea carbon sequestration leakage. *Limnol. Oceanogr.* 60, 402–410.
- Breuer, E., Stevenson, A.G., Howe, J.A., Carroll, J., Shimmield, G.B., 2004. Drill cutting accumulations in the Northern and Central North Sea: a review of environmental interactions and chemical fate. *Mar. Pollut. Bull.* 48, 12–25.
- Cazenave, P., Torres, R., Blackford, J., Artioli, Y., Bruggeman, J., 2018. Regional Modelling to Inform the Design of Sub-Sea CO<sub>2</sub> Storage Monitoring Networks. Social Science Research Network, Rochester, NY.
- Cefas Data Hub, 2020. Cefas - Sea Temperature and Salinity Trends. Database available online: <https://www.cefas.co.uk/cefas-data-hub/sea-temperature-and-salinity-trends/>.
- Clayton, T.D., Byrne, R.H., 1993. Spectrophotometric seawater pH measurements: total hydrogen ion concentration scale calibration of m-cresol purple and at-sea results. *Deep. Sea Res. Part I Oceanogr. Res. Pap.* 40, 2115–2129.

- Clinton-Bailey, G.S., Grand, M.M., Beaton, A.D., Nightingale, A.M., Owsianka, D.R., Slavik, G.J., Connelly, D.P., Cardwell, C.L., Mowlem, M.C., 2017. A lab-on-chip analyzer for in situ measurement of soluble reactive phosphate: improved phosphate blue assay and application to fluvial monitoring. *Environ. Sci. Technol.* 51, 9989–9995.
- Connelly, D., 2019. JC180 cruise report- strategies for the environmental monitoring of Marine carbon capture and storage. STEMM-CCS April 25<sup>th</sup> 2019 - May 30<sup>th</sup> 2019 Southampton - Aberdeen - Southampton, NOC Reports. National Oceanography Centre, Southampton, UK.
- Cotton, A., Gray, L., Maas, W., 2017. Learnings from the shell peterhead CCS project front end engineering design. *Energy Procedia* 114, 5663–5670.
- Dale, A.W., Nickelsen, L., Scholz, F., Hensen, C., Oeschies, A., Wallmann, K., 2015. A revised global estimate of dissolved iron fluxes from marine sediments. *Global Biogeochem. Cycles* 29, 691–707.
- Dale, A.W., Sommer, S., Lichtschlag, A., Koopmans, D., Haeckel, M., Kossel, E., Deuser, C., Linke, P., Scholten, J., Wallmann, K., van Erk, M., Gros, J., Scholz, F., Schmidt, M., 2020. Defining a biogeochemical baseline for sediments at Carbon Capture and Storage (CCS) sites: an example from the North Sea (Goldeneye). *Int. J. Greenh. Gas Control*. This issue Submitted for publication.
- de Beer, D., 2000. Potentiometric microsensors for in situ measurements in aquatic environments. In: Buffle, J., Horvai, G. (Eds.), *In Situ Monitoring of Aquatic Systems: Chemical Analysis and Speciation*. Wiley & Sons, London, pp. 161–194.
- de Beer, D., Lichtschlag, A., Flohr, A., van Erk, M.R., Ahmerkamp, S., Holtappels, M., Haeckel, M., Strong, J., 2021. Sediment acidification and temperature increase in an artificial CO<sub>2</sub> vent. *Int. J. Greenh. Gas Control* 105, 103244.
- Dean, M., Tucker, O., 2017. A risk-based framework for Measurement, Monitoring and Verification (MMV) of the Goldeneye storage complex for the Peterhead CCS project, UK. *Int. J. Greenh. Gas Control* 61, 1–15.
- Dewar, M., Sellami, N., Chen, B., 2015. Dynamics of rising CO<sub>2</sub> bubble plumes in the QICS field experiment: part 2 – modelling. *Int. J. Greenh. Gas Control* 38, 52–63.
- Dickson, A.G., Sabine, C.L., Christian, J.R., 2007. *Guide to Best Practices for Ocean CO<sub>2</sub> Measurements*. North Pacific Marine Science Organization.
- Dixon, T., Romanak, K.D., 2015. Improving monitoring protocols for CO<sub>2</sub> geological storage with technical advances in CO<sub>2</sub> attribution monitoring. *Int. J. Greenh. Gas Control* 41, 29–40.
- Dlugokencky, E., Tans, P.P., 2020. Trends in Atmospheric CO<sub>2</sub>, National Oceanic & Atmospheric Administration, Earth System Research Laboratory (NOAA/ESRL). Available at: <http://www.esrl.noaa.gov/gmd/ccgg/trends/global.html>, last access: 1 May 2020. NOAA/ESRL.
- Esposito, M., Martínez-Cabanas, M., Connelly, D.P., Jasinski, D., Linke, P., Schmidt, M., Achterberg, E.P., 2020. Water column baseline assessment for offshore Carbon Dioxide Capture and Storage (CCS) sites: analysis of field data from the Goldeneye storage complex area. *Int. J. Greenh. Gas Control*. This issue Submitted for publication.
- EU, 2009. Implementation of directive 2009/31/EC on the geological storage of carbon dioxide. *Guidance Documents*, pp. 1–4.
- Flohr, A., Matter, J.M., James, R.H., Saw, K., Brown, R., Ballentine, C.J., Day, C., Connelly, D., Flude, S., Gros, J., Hillegonds, D.J., Lichtschlag, A., Pearce, C.R., Peel, K., Strong, James, Tyne, R.L., 2020. Utility of natural and artificial geochemical tracers for leakage monitoring and quantification during an offshore controlled CO<sub>2</sub> release experiment. *Int. J. Greenh. Gas Control*. This issue Submitted for publication.
- Friedlingstein, P., Jones, M.W., O'Sullivan, M., Andrew, R.M., Hauck, J., Peters, G.P., et al., 2019. *Global carbon budget 2019*. *Earth Syst. Sci. Data* 11, 1783–1838.
- Furre, A.-K., Eiken, O., Alnes, H., Veatne, J.N., Kier, A.F., 2017. 20 years of monitoring CO<sub>2</sub>-injection at Sleipner. *Energy Procedia* 114, 3916–3926.
- Gates, A.R., Jones, D.O.B., 2012. Recovery of benthic megafauna from anthropogenic disturbance at a hydrocarbon drilling well (380 m depth in the Norwegian Sea). *PLoS One* 7.
- German, C., Tyler, P., Griffiths, G., 2003. The maiden voyage of UK ROV "Isis". *Ocean Challenge* 12, 16–18.
- Gieseke, A., de Beer, D., 2004. Use of microelectrodes to measure in situ microbial activities in biofilms, sediments, and microbial mats. In: Akkermans, A.D.L., van Elsas, D. (Eds.), *Molecular Microbial Ecology Manual*, 2 ed. Kluwer, Dordrecht, pp. 1581–1612.
- GLODAP Reference Group, 2020. *Global Ocean Data Analysis Project Version 2*. Database available online: <https://www.glodap.info/>.
- Grasshoff, K., Kremling, K., Ehrhardt, M., 1999. *Methods of Seawater Analysis*, 1 ed. John Wiley & Sons, Ltd.
- Grassle, J.F., Sanders, H.L., Hessler, R.R., Rowe, G.T., McLellan, T., 1975. Pattern and zonation: a study of the bathyal megafauna using the research submersible Alvin. *Deep. Sea Res. Oceanogr. Abstr.* 22, 457–481.
- Greenwood, J., Craig, P., Hardman-Mountford, N., 2015. Coastal monitoring strategy for geochemical detection of fugitive CO<sub>2</sub> seeps from the seabed. *Int. J. Greenh. Gas Control* 39, 74–78.
- Gros, J., Schmidt, M., Dale, A.W., Linke, P., Vielstädte, L., Bigalke, N., Haeckel, M., Wallmann, K., Sommer, S., 2019. Simulating and quantifying multiple natural subsea CO<sub>2</sub> seeps at Panarea Island (Aeolian Islands, Italy) as a proxy for potential leakage from subseabed carbon storage sites. *Environ. Sci. Technol.* 53, 10258–10268.
- Gros, J., Schmidt, M., Linke, P., Dötsch, S., Triest, J., Martínez-Cabanas, M., Esposito, M., Dale, A.W., Sommer, S., Flohr, A., Fone, J., Bull, J.M., Roche, B., Strong, J.A., Saw, K., Brown, R., Koopmans, D., Wallman, K., 2020. Quantification of dissolved CO<sub>2</sub> plumes at the Goldeneye CO<sub>2</sub>-release experiment. *Int. J. Greenh. Gas Control*. This issue Submitted for publication.
- Gundersen, C., Oleynik, A., Alendal, G., Skaug, H.J., Avlesen, H., Berntsen, J., Blaser, N., Blackford, J., Cazenave, P., 2018. Ensuring efficient and robust offshore storage – use of models and machine learning techniques to design leak detection monitoring. In: 14th International Conference on Greenhouse Gas Control Technologies, GHGT-14, 21st–25th October 2018. Melbourne, Australia.
- Hansen, H.P., Koroleff, F., 2007. *Determination of nutrients, Methods of Seawater Analysis*. John Wiley & Sons, Ltd, pp. 159–228.
- Hansen, O., Gilding, D., Nazarian, B., Osdal, B., Ringrose, P., Kristoffersen, J.-B., Eiken, O., Hansen, H., 2013. Snøhvit: the history of injecting and storing 1 Mt CO<sub>2</sub> in the Fluvial Tubåen Fm. *Energy Procedia* 37, 3565–3573.
- Hepple, R.P., Benson, S.M., 2005. Geologic storage of carbon dioxide as a climate change mitigation strategy: performance requirements and the implications of surface seepage. *Environ. Geol.* 47, 576–585.
- Hosking, B., Horton, T., Durden, J.M., Jones, D.O.B., Ruhl, H.A., 2020. Benthic megafaunal specimen counts from seabed photographs at a site in the Central North Sea (STEMM-CCS Project). *Pangaea*. <https://doi.org/10.1594/PANGAEA.912668>.
- Hvidevold, H.K., Alendal, G., Johannessen, T., Ali, A., Mannseth, T., Avlesen, H., 2015. Layout of CCS monitoring infrastructure with highest probability of detecting a footprint of a CO<sub>2</sub> leak in a varying marine environment. *Int. J. Greenh. Gas Control* 37, 274–279.
- Hvidevold, H.K., Alendal, G., Johannessen, T., Ali, A., 2016. Survey strategies to quantify and optimize detecting probability of a CO<sub>2</sub> seep in a varying marine environment. *Environ. Model. Softw.* 83, 303–309.
- IEAGHG, 2008. *Assessment of Sub Sea Ecosystem Impacts*. EA Greenhouse Gas R&D programme.
- IEAGHG, 2012. *Quantification Techniques for CO<sub>2</sub> Leakage*, 2012/02, January, 2012.
- IEAGHG, 2015. *Review of Offshore Monitoring for CCS Projects*, 2015/02, July 2015.
- IMO, 2006. 2006 Amendment of 1996 Protocol to the Convention on the Prevention of Marine Pollution by Dumping of Wastes and Other Matter, p. 1972.
- IPCC, 2005. In: Metz, B., Davidson, O., de Coninck, H.C., Loos, M., Meyer, L.A. (Eds.), *Special Report on Carbon Dioxide Capture and Storage*. Prepared by Working Group III of the Intergovernmental Panel on Climate Change. IPCC, Cambridge University Press, The Edinburgh Building Shaftesbury Road, Cambridge, England.
- IPCC, 2014. *Climate change 2014: synthesis report*. In: Core Writing Team, Pachauri, R. K., Meyer, L.A. (Eds.), *Contribution of Working Groups I, II and III to the Fifth Assessment Report of the Intergovernmental Panel on Climate Change*. IPCC, Geneva, Switzerland.
- IPCC, 2018. *Summary for policymakers*. In: Masson-Delmotte, V., Zhai, P., Pörtner, H.-O., Roberts, D., Skea, J., Shukla, P.R., Pirani, A., Moufouma-Okia, W., Péan, C., Pidcock, R., Connors, S., Matthews, J.B.R., Chen, Y., Zhou, X., Gomis, M.I., Lonnoy, E., Maycock, T., Tignor, M., Waterfield, T. (Eds.), *Global Warming of 1.5°C*. An IPCC Special Report on the Impacts of Global Warming of 1.5°C Above pre-Industrial Levels and Related Global Greenhouse Gas Emission Pathways, in the Context of Strengthening the Global Response to the Threat of Climate Change, Sustainable Development, and Efforts to Eradicate Poverty. World Meteorological Organization, Geneva, Switzerland, 32 pp.
- Jenkins, C., Chadwick, A., Hovorka, S.D., 2015. The state of the art in monitoring and verification—ten years on. *Int. J. Greenh. Gas Control* 40, 312–349.
- Jørgensen, B.B., Revsbech, N.P., 1985. Diffusive boundary layers and the oxygen uptake of sediments and detritus. *Limnol. Oceanogr.* 30, 111–122.
- Jones, D.O.B., Gates, A.R., Lausen, B., 2012. Recovery of deep-water megafaunal assemblages from hydrocarbon drilling disturbance in the Faroe–Shetland Channel. *Mar. Ecol. Prog. Ser.* 461, 71–82.
- Jones, D.G., Beaubien, S.E., Blackford, J.C., Foekema, E.M., Lions, J., De Vittor, C., West, J.M., Widdicombe, S., Hauton, C., Queirós, A.M., 2015. Developments since 2005 in understanding potential environmental impacts of CO<sub>2</sub> leakage from geological storage. *Int. J. Greenh. Gas Control* 40, 350–377.
- Karstens, J., Böttner, C., Edwards, M., Falcon-Suarez, I., Flohr, A., James, R., Lichtschlag, A., Maicher, D., Pheasant, I., Roache, B., Schramm, B., Wilson, M., 2019. *RV MARIA S. MERIAN Fahrtbericht/Cruise Report MSM78-PERMO 2*, Edinburgh–Edinburgh (UK), 16.10.–25.10. p. 2018.
- Klimant, I., Huber, C., Liebsch, G., Neuraüter, G., Stangelmayer, A., Wolfbeis, O.S., 2001. Dual lifetime referencing (DLR) — a New Scheme for converting fluorescence intensity into a frequency-domain or time-domain information. In: Valeur, B., Brochon, J.-C. (Eds.), *New Trends in Fluorescence Spectroscopy: Applications to Chemical and Life Sciences*. Springer, Berlin, Heidelberg, pp. 257–274.
- Koopmans, D., Meyer, V., Schaap, A., Dewar, M., Färber, P., Long, M., Connelly, D., Holtappels, M., 2020. Detection and quantification of a release of carbon dioxide gas from the seafloor using pH eddy covariance and mass transport. *Int. J. Greenh. Gas Control*. This issue Submitted for publication.
- Kühl, M., Revsbech, N., 2001. Biogeochemical microsensors for boundary layer studies. In: Boudreau, B., Jørgensen, B.B. (Eds.), *The Benthic Boundary Layer*. Oxford University Press, pp. 180–210.
- Langenkämper, D., Zurowicz, M., Schoening, T., Nattkemper, T.W., 2017. BIIGLE 2.0 - browsing and annotating large marine image collections. *Front. Mar. Sci.* 4.
- Law, A., Raymond, A., White, G., Atkinson, A., Clifton, M., Atherton, T., Dawes, I., Robertson, E., Melvi, A., Brayley, S., 2000. The Kopervik fairway, Moray Firth, UK. *Pet. Geosci.* 6, 265–274.
- Leighton, T.G., White, P.R., 2012. Quantification of undersea gas leaks from carbon capture and storage facilities, from pipelines and from methane seeps, by their acoustic emissions. *Proceed. R. Soc. A: Math. Phys. Eng. Sci.* 468, 485–510.
- Lessin, G., Artioli, Y., Queirós, A.M., Widdicombe, S., Blackford, J.C., 2016. Modelling impacts and recovery in benthic communities exposed to localised high CO<sub>2</sub>. *Mar. Pollut. Bull.* 109, 267–280.
- Lessin, G., Artioli, Y., Bruggeman, J., Blackford, J., 2018. Can We Use Departure from Natural Co-Variance Relationships for Monitoring of Offshore Carbon Storage Integrity? *Social Science Research Network*, Rochester, NY.



- Li, J., White, P.R., Bull, J.M., Leighton, T.G., 2019. A noise impact assessment model for passive acoustic measurements of seabed gas fluxes. *Ocean. Eng.* 183, 294–304.
- Li, J., Roche, B., Bull, J.M., White, P.R., Davis, J.W., Deponte, M., Gordini, E., Cotterle, D., 2020. Passive acoustic monitoring of a natural CO<sub>2</sub> seep site – Implications for carbon capture and storage. *Int. J. Greenh. Gas Control*. This issue.
- Lichtschiag, A., Haeckel, M., Ollirook, D., Peel, K., Flohr, A., Pearce, C.R., James, R.H., Marieni, C., Connelly, D.P., 2020a. Impact of CO<sub>2</sub> leakage from sub-seabed carbon dioxide storage on sediment and porewater geochemistry. *Int. J. Greenh. Gas Control*. This issue. Submitted for publication.
- Lichtschiag, A., Pearce, C., Suominen, M., Blackford, J.C., Borisov, S., Bull, J., de Beer, D., Dean, M., Flohr, A., Esposito, M., Gros, J., Haeckel, M., Huvenne, V., James, R., Koopmans, D., Linke, P., Mowlem, M., Omar, A., Schaap, A., Schmidt, M., Sommer, S., Strong, J., Connelly, D., 2020b. Suitability analysis and revised strategies for marine environmental carbon capture and storage (CCS) monitoring. *Int. J. Greenh. Gas Control*. This issue. Submitted for publication.
- Linke, P., Haeckel, M., 2018. RV POSEIDON Fahrtbericht / Cruise Report POS518: Baseline Study for the Environmental Monitoring of Subseafloor CO<sub>2</sub> Storage Operations, Leg 1: Bremerhaven – Bremerhaven (Germany) 25.09.–11.10.2017, Leg 2: Bremerhaven – Kiel (Germany) 12.10.–28.10.2017. GEOMAR Helmholtz-Zentrum für Ozeanforschung, Kiel.
- Long, M.H., Charette, M.A., Martin, W.R., McCorkle, D.C., 2015. Oxygen metabolism and pH in coastal ecosystems: eddy Covariance Hydrogen ion and Oxygen Exchange System (ECHOES). *Limnol. Oceanogr. Methods* 13, 438–450.
- Mabon, L., Shackley, S., Bower-Bir, N., 2014. Perceptions of sub-seabed carbon dioxide storage in Scotland and implications for policy: a qualitative study. *Mar. Policy* 45, 9–15.
- Mabon, L., Shackley, S., Blackford, J.C., Stahl, H., Miller, A., 2015. Local perceptions of the QICS experimental offshore CO<sub>2</sub> release: results from social science research. *Int. J. Greenh. Gas Control* 38, 18–25.
- Mabon, L., Kita, J., Xue, Z., 2017. Challenges for social impact assessment in coastal regions: a case study of the Tomakomai CCS demonstration project. *Mar. Policy* 83, 243–251.
- Martínez-Cabanas, M., Esposito, M., Gros, J., Linke, P., Schmidt, M., Triest, J., Achterberg, E., 2020. Deviations from environmental baseline: Detection of subsea CO<sub>2</sub> release in the water column from real-time measurements at a potential offshore carbon dioxide storage site. *Int. J. Greenh. Gas Control*. This issue Submitted for publication.
- McGinnis, D.F., Schmidt, M., DelSontro, T., Themann, S., Rovelli, L., Reitz, A., Linke, P., 2011. Discovery of a natural CO<sub>2</sub> seep in the German North Sea: implications for shallow dissolved gas and seep detection. *J. Geophys. Res.* Oceans 116, C03013.
- McGinnis, D.F., Sommer, S., Lorke, A., Glud, R.N., Linke, P., 2014. Quantifying tidally driven benthic oxygen exchange across permeable sediments: an aquatic eddy correlation study. *J. Geophys. Res.* Oceans 119, 6918–6932.
- Monk, S., Schaap, A., Hanz, R., Borisov, S., Loucaides, S., Arundell, M., Papadimitriou, S., Walk, J., Tong, D., Wyatt, J., Mowlem, M., 2020. Detecting and mapping a CO<sub>2</sub> plume with novel autonomous pH sensors on an underwater vehicle. *Int. J. Greenh. Gas Control*. This issue Submitted for publication.
- Montserrat, F., Van Colen, C., Provoost, P., Milla, M., Ponti, M., Van den Meersche, K., Ysebaert, T., Herman, P.M.J., 2009. Sediment segregation by biodiffusing bivalves. *Estuar. Coast. Shelf Sci.* 83, 379–391.
- Murphy, J., Riley, J.P., 1962. A modified single solution method for the determination of phosphate in natural waters. *Anal. Chim. Acta* 27, 31–36.
- Oleynik, A., Gundersen, C., Alendal, G., Skaug, H.J., Gullikson, M., Avlesen, H., Berntsen, J., Blackford, J., Cazenave, P., 2018. Simplified modeling as a tool to locate and quantify fluxes from CO<sub>2</sub> seep to marine waters. In: 14th International Conference on Greenhouse Gas Control Technologies, GHGT-14, 21st–25th October 2018. Melbourne, Australia.
- Oleynik, A., García-Ibáñez, M.I., Blaser, N., Omar, A., Alendal, G., 2020. Optimal sensors placement for detecting CO<sub>2</sub> discharges from unknown locations on the seafloor. *Int. J. Greenh. Gas Control* 95, 102951.
- Omar, A.M., García-Ibáñez, M.I., Schaap, A., Oleynik, A., Esposito, M., Jeansson, E., Loucaides, S., Thomas, H., Alendal, G., 2020. Detection and quantification of CO<sub>2</sub> seepage in seawater using the stoichiometric Cseep method: results from a recent subsea CO<sub>2</sub> release experiment in the North Sea. *Int. J. Greenh. Gas Control*. This issue Submitted for publication.
- OSPAR, 2007. 2007 Amendment to 1992 OSPAR Convention, Convention for the Protection of the Marine Environment of the North-East Atlantic.
- Rérolle, V.M.C., Floquet, C.F.A., Harris, A.J.K., Mowlem, M.C., Bellerby, R.R.G.J., Achterberg, E.P., 2013. Development of a colorimetric microfluidic pH sensor for autonomous seawater measurements. *Anal. Chim. Acta* 786, 124–131.
- Revsbech, N.P., Jørgensen, B.B., 1986. Microelectrodes: their use in microbial ecology. In: Marshall, K.C. (Ed.), *Advances in Microbial Ecology*. Springer US, Boston, MA, pp. 293–352.
- Ringrose, P.S., Meckel, T.A., 2019. Maturing global CO<sub>2</sub> storage resources on offshore continental margins to achieve 2DS emissions reductions. *Sci. Rep.* 9, 17944.
- Robinson, A.H., Callow, B., Böttner, C., Yilo, N., Provenzano, G., Falcon-Suarez, I.H., Marín-Moreno, H., Lichtschlag, A., Bayrakci, G., Gehrman, R., Parkes, L., Roche, B., Saleem, U., Schramm, B., Waage, M., Lavayssière, A., Li, J., Jedari-Eyvazi, F., Sahoo, S., Deusner, C., Kossel, E., Minshull, T.A., Berndt, C., Bull, J.M., Dean, M., James, R.H., Chapman, M., Best, A.I., Büinz, S., Chen, B., Connelly, D.P., Elger, J., Haeckel, M., Henstock, T.J., Karstens, J., Macdonald, C., Matter, J.M., North, L., Reinardy, B., 2020. Multiscale characterisation of chimneys/pipes: fluid escape structures within sedimentary basins. *Int. J. Greenh. Gas Control*. This issue Submitted for publication.
- Roche, B., Bull, J.M., Marín-Moreno, H., Leighton, T.G., Falcon-Suarez, I.H., White, P.G., Provenzano, G., Tholen, M., Lichtschlag, A., Li, J., Fagetter, M., 2020. Time-lapse imaging of CO<sub>2</sub> migration within near-surface sediments during a controlled sub-seabed release experiment. *Int. J. Greenh. Gas Control*. This issue Submitted for publication.
- Schaap, A., Koopmans, D., Holtappels, M., Dewar, M., Arundell, M., Papadimitriou, S., Hanz, R., Monk, S., Mowlem, M., Loucaides, S., 2020. Quantification of a subsea CO<sub>2</sub> release with lab-on-chip sensors measuring benthic gradients. *Int. J. Greenh. Gas Control*. This issue Submitted for publication.
- Schmidt, M., 2019. RV POSEIDON Fahrtbericht / Cruise Report POS534 Leg 1: Kiel (Germany) – Aberdeen (United Kingdom) 01.05. – 22.05.2019 Leg 2: Aberdeen (United Kingdom) – Bremerhaven (Germany) 23.05. – 29.05.2019, GEOMAR Report. GEOMAR Helmholtz-Zentrum für Ozeanforschung, Kiel, Germany, p. 51.
- Schmidt, M., Linke, P., Sommer, S., Esser, D., Cherednichenko, S., 2015. Natural CO<sub>2</sub> seeps offshore panarea: a test site for subsea CO<sub>2</sub> leak detection technology. *Mar. Technol. Soc. J.* 49, 19–30.
- Schmidt, M., Esposito, M., Gros, J., Kossel, E., Mesher, T., Durden, J.M., Deusner, C., Koopmans, D., de Beer, D., Flohr, A., Dale, A., Linke, P., Haeckel, M., Triest, J., Elsen, S., Somerfield, P., McNeill, C.L., Rühl, S., Jones, D.O.B., Huvenne, V., Achterberg, E., Wallmann, K., Widdicombe, S., 2020. Report for STEMM Deliverable 2.8: Observation Data Synthesis (Baseline), Including Water Column Chemistry, Geochemical Fluxes and Benthic Biota. Available online at: <https://cordis.europa.eu/project/id/654462/results>.
- Shell, U.K., 2015. Shell: Storage Development Plan - Peterhead CCS Project. DECC\_11.128.KKD Subsurface. Available online, p. 2015 [https://www.gov.uk/government/uploads/system/uploads/attachment\\_data/file/531016/DECC\\_Ready\\_-\\_KKD\\_11.128.Storage\\_Development\\_Plan.pdf](https://www.gov.uk/government/uploads/system/uploads/attachment_data/file/531016/DECC_Ready_-_KKD_11.128.Storage_Development_Plan.pdf).
- Sommer, S., Schmidt, M., Linke, P., 2015. Continuous inline mapping of a dissolved methane plume at a blowout site in the Central North Sea UK using a membrane inlet mass spectrometer – water column stratification impedes immediate methane release into the atmosphere. *Mar. Pet. Geol.* 68, 766–775.
- Sommer, S., Gier, J., Treude, T., Lomnitz, U., Dengler, M., Cardich, J., Dale, A.W., 2016. Depletion of oxygen, nitrate and nitrite in the Peruvian oxygen minimum zone cause an imbalance of benthic nitrogen fluxes. *Deep-Sea Res. Part I* 112, 113–122.
- Staudinger, C., Strobl, M., Breininger, J., Klimant, I., Borisov, S.M., 2019. Fast and stable optical pH sensor materials for oceanographic applications. *Sens. Actuators B Chem.* 282, 204–217.
- STEMM-CCS D2.7, 2020. Report for STEMM Deliverable 2.7: Environmental Baseline Data. Available online at: <https://cordis.europa.eu/project/id/654462/results>.
- Strong, J.A., Huvenne, V.A.L., Mesher, T., Somerfield, P., Tilstone, G.H., Wardell, C., Widdicombe, S., Le Bas, T.P., Lo Iacono, C., Pearce, C.R., Connelly, D., 2020. Environmental description of the STEMM-CCS experimental site and surrounding area. *Int. J. Greenh. Gas Control*. This issue Submitted for publication.
- Taylor, P., Stahl, H., Vardy, M.E., Bull, J.M., Akhurst, M., Hauton, C., James, R.H., Lichtschlag, A., Long, D., Aleynik, D., Toberman, M., Naylor, M., Connelly, D., Smith, D., Sayer, M.D.J., Widdicombe, S., Wright, I.C., Blackford, J., 2015. A novel sub-seabed CO<sub>2</sub> release experiment informing monitoring and impact assessment for geological carbon storage. *Int. J. Greenh. Gas Control, CCS Mar. Environ.* 38, 3–17.
- UNFCCC, 2015. In: United Nations / Framework Convention on Climate Change, Adoption of the Paris Agreement, 21st Conference of the Parties. Paris.
- Van der Meer, L.G.H., 2013. 13 - the K12-B CO<sub>2</sub> injection project in the Netherlands. In: Gluyas, J., Mathias, S. (Eds.), *Geological Storage of Carbon Dioxide (CO<sub>2</sub>)*. Woodhead Publishing, pp. 301–332e.
- Van Hoey, G., Guilini, K., Rabaut, M., Vincx, M., Degraer, S., 2008. Ecological implications of the presence of the tube-building polychaete *Lanice conchilega* on soft-bottom benthic ecosystems. *Mar. Biol.* 154, 1009–1019.
- Vandeweyer, V., van der Meer, B., Hofstee, C., Mulders, F., D’Hoore, D., Graven, H., 2011. Monitoring the CO<sub>2</sub> injection site: K12-B. *Energy Procedia* 4, 5471–5478.
- Vangkilde-Pederson, T., 2009. GeoCapacity Project. D 16 WP2 Report: Storage Capacity Deliverable Report for the EU GeoCapacity Project.
- Vielstädte, L., Linke, P., Schmidt, M., Sommer, S., Haeckel, M., Braack, M., Wallmann, K., 2019. Footprint and detectability of a well leaking CO<sub>2</sub> in the Central North Sea: implications from a field experiment and numerical modelling. *Int. J. Greenh. Gas Control* 84, 190–203.
- Widdicombe, S., Huvenne, V., Strong, J., Blackford, J., Tilstone, G., 2018. Establishing an Effective Environmental Baseline for Offshore CCS, 14th Greenhouse Gas Control Technologies Conference (GHGT-14).
- Wilson, J., Wall, G., Kloosterman, H.J., Coney, D., Cayley, G., Walker, J., Linskaill, C., 2005. The discovery of Goldeneye: Kopervik prospect and play mapping in the South Halibut Basin of the Moray Firth. In: *Geological Society, London, Petroleum Geology Conference Series*, 6, pp. 199–216.
- Zeebe, R.E., Wolf-Gladrow, D.A., 2001. CO<sub>2</sub> in seawater: Equilibrium, Kinetics, Isotopes, 1st ed. Elsevier Science.
- Zurawietz, M., Langenkämper, D., Hosking, B., Rühl, H.A., Nattkemper, T.W., 2018. MAIA—a machine learning assisted image annotation method for environmental monitoring and exploration. *PLoS One* 13.